DEVELOPMENT OF A THERMODYNAMIC MODEL FOR FLUIDS CONFINED IN SPHERICAL PORES

A Thesis

by

MICHELLE LYNN D'LIMA

Submitted to the Office of Graduate and Professional Studies of
Texas A&M University
in partial fulfillment of the requirements for the degree of

MASTER OF SCIENCE

Chair of Committee,	Marcelo Castier
Committee Members,	Kenneth Hall
	Michael Fraim
Head of Department,	M. Nazmul Karim

August 2014

Major Subject: Chemical Engineering

ABSTRACT

The thermodynamic properties of a fluid confined in extremely small pores can be substantially different from those observed of the same bulk fluid. These differences in behavior could have technical applications in adsorption-based separations; may pose a challenge with regards to the extraction of oil entrapped in the small cavities of reservoir rocks; or could even be utilized in complex heterogeneous catalytic systems such as those used in gas-to liquid fuel conversions.

This thesis describes the use of the generalized van der Waals theory to extend cubic equations of state, such as Peng-Robinson, that are widely applied in the oil and gas industry to model the behavior of pure fluids as well as mixtures confined in spherical pores. Empirical expressions were developed for the coordination number in spherical pores as a function of the molecule to pore size ratio, for the distribution of molecules along the pore radius as function of temperature, and of the interaction potential between the molecules and the pore wall. Despite their relative simplicity, the expressions capture the limiting behaviors expected at high and low temperatures. The model parameters were then fitted to experimental data for the adsorption of light hydrocarbons and gases in common adsorbents. Finally, the calculated results were compared to the experimental results in order to assess the performance of the model, through adsorption equilibrium calculations.

ACKNOWLEDGEMENTS

I would like to thank my committee chair, Dr. Marcelo Castier, and my committee members, Dr. Kenneth Hall and Dr. Michael Fraim for their guidance and support throughout the course of this research. I would like to specially thank Dr. Ricardo F. Checoni and Dr. Leonardo Travalloni for their constant input and support.

Thanks also go to my friends and colleagues and the department faculty and staff for making my time at Texas A&M University at Qatar so memorable. Special thanks go out to Mr. Rithwick Varier, B.Sc. and Mr. Sudeep Gowrishankar, M.Sc., from the University of Illinois at Urbana Champaign for their helpful advice as well as their constant support throughout the writing process. Finally, I would like to thank my mom, dad and sister for their constant support and encouragement. Without them, I would not be where I am today.

This thesis was made possible by a NPRP award [NPRP 5-344-2-129] from the Qatar National Research Fund (a member of The Qatar Foundation). The statements made herein are solely the responsibility of the author.

NOMENCLATURE

a_i	Energy parameter of pure component *i*
a_p	Confinement-modified energy parameter of the equation of state
$a_{p,ij}$	Confinement-modified energy parameter for a mixture
b_i	Volume parameter of pure component *i*
b_p	Confinement-modified volume parameter of the equation of state
$b_{p,i}$	Confinement-modified volume parameter of pure component *i*
E_{conf}	Configurational energy
F_p	Fraction of the confined molecules subject to the pore wall attractive field for random distribution of the molecules inside the pore
$f_{w,i}$	Parameter used in a_i
k	Boltzmann constant
N	Total number of molecules
N_{av}	Avogadro's number
P	Pressure

q	Internal partition function of one molecule
Q	Canonical partition function
R	Ideal gas constant
r_p	Pore radius
T	Absolute temperature
V	Total volume
V_f	Free volume
A_n	Lower asymptote
K_n	Upper asymptote
B_n	Growth rate
Q_n	Depends on the value of the average logistic function at t = 0
M_n	Time of maximum growth if $Q = \eta$
W	Value of the average logistic function divided by 10
η_n	Affects near which asymptote maximum growth occurs in the normal distribution function
σ_n	Standard deviation parameter in the normal distribution function

μ_n	Mean or expectation of the normal distribution function
δ_p	Square well width of the molecule-wall interaction potential
ε_p	Square well depth of the molecule-wall interaction potential
λ	De Broglie wavelength
ρ_{max}	Confinement-modified number packing density
$\rho_{n,\max}$	Confinement-modified molar packing density
σ	Molecular diameter
ν	Molar volume
ω	Accentric factor
i,j	Components
NC	Number of fluid components

TABLE OF CONTENTS

Page

LIST OF FIGURES

Page

LIST OF TABLES

Page

CHAPTER I

INTRODUCTION

It is a well-known fact that the behavior of fluids confined within small pores highly differs from regular behavior in the bulk phase. This phenomenon is more pronounced when the size of the pore is in the range of nanometers, and the effects of constraint as well as the interaction between the pore wall and the molecule of the fluid must be taken into account. Modeling of this kind of phenomenon is extremely important for the chemical industry, as many operations and processes involve confined fluids. Another complexity associated with modeling the adsorption of a system is a lack of representation of structural heterogeneity or whether the adsorbent can influence the behavior of the system.

The difference between fluid properties in the bulk phase and the confined phase depends on the interaction of fluid molecules with the wall of the porous media that entraps them. Current adsorption models often do not include the effect of adsorbent pore size and shape, accounting for only the chemical heterogeneity aspect of the surface. Hence there is a need to study the effects of pore size and shape on confinement. This can be done in great detail using molecular simulations. However, the downside to utilizing such simulations is that their computational demand proves to be too high for practical equipment and process design.

The development of such models can help predict the behavior of confined fluids in the applications of heterogeneous catalysis. Warrag[1] applied an equation of state for

fluids confined in cylindrical pores, developed by Travalloni et al[2], to investigate possible fluid condensation inside the pores of the catalysts employed in the Fischer Tropsch synthesis, as part of the Gas-to-Liquids process. Multi-phase equilibrium calculations were also performed for the bulk and confined regions of the catalyst.

A model that can describe the phenomena of confinement would be highly pertinent to the field of Oil & Gas for application to oil deposits confined in porous rocks in reservoirs. The oil extraction process is complicated, due to the complexity of the fluid mixture as well as due to the properties of the porous media in which it is entrapped. Most water and hydrocarbon systems display three phases, namely an organic liquid phase, an aqueous phase, and a gaseous phase, with flat phase interfaces. However, this generalization cannot be applied to most petroleum reservoirs. In reality, there are transition regions in which several phases can exist, namely water-oil contact (WOC) regions and gas-oil contact (GOC) regions. The compositions of these phases can differ, i.e. within the same reservoir, the confined fluid may be in either liquid or vapor phase, depending on the nature of the adsorbent that the particles are confined in. Another aspect that adds to the complexity of these calculations is that the composition of a phase may vary for different pores. Hence a model that can simultaneously predict the effect of height and confinement can be utilized in predicting the occurrence of WOC and GOC regions.

Continuing previous work of our group on the behavior of confined fluids, the objective is to develop a thermodynamic model for fluids confined in spherical pores.

This thesis will extend the Peng-Robinson equation of state to this case, through use of the generalized van der Waal's theory as a starting point for the model's derivation.

Using the existing equation of state for cylindrical pores as a basis, this expression can be modified for spherical pores. This can be accomplished by developing expressions for the porosity and coordination number, as well as modifying the configurational energy expression and the free volume expression to account for spherical geometry. The modified Peng-Robinson equation of state models the fluid in bulk and confined spaces, thus it presents itself as a practical approach to describe confinement. The bulk phase is treated a system confined by an extremely large pore so that the effect of the wall on the molecules is negligible.

An advantage of using the same model for both bulk and confined phases is the ease of modification of conventional phase equilibrium procedures and computational programs to account for confinement. From a theoretical standpoint, this particular approach ensures consistent representation of fluid behavior over wide ranges of pressure. From a practical view, this technique enables ease of adaptation of existing computational procedures for phase equilibrium calculations in the cases of adsorption, such as the dew point, bubble point and flash point. It also greatly simplifies the computation of the calorimetric properties of adsorption. Another added benefit of this model is the relative simplicity of the mathematical calculations.

The structure of this thesis is described as follows. Chapter II presents a literature review on the history of thermodynamics and cubic equations of state and the development of models related to confinement of fluids. Chapter III discusses the

theoretical basis and the simplifying assumptions adopted in this work for the development of equations of state for pure fluids and confined mixtures, as well as the formulation of the model obtained. Chapter IV discusses the different kinds of porous adsorbents that have a spherical structure, and can be considered for applications of the model. Chapter V presents the equilibrium calculations and the parametric fitting methods that were utilized in the analysis of the developed model, in order to obtain a conclusive comparison between experimental and calculated results. Chapter VI discusses the results of the evaluated model, and what adjustments could be made to improve it. Chapter VII presents the conclusions of this work and Chapter VIII contains information regarding the continuity of this work and future areas that need to be investigated.

CHAPTER II

LITERATURE REVIEW

Previous work on the development of an equation of state to calculate the properties of confined fluids has been carried out. Zhu *et al.*[3] developed an equation of state for fluids confined in cylindrical pores from the formulation of a theory of interfaces, based on the attractive interactions between the adsorbent and adsorbed phases, as well as the concepts of surface tension and curvature of the adsorbed interface. The fluid pressure in the pore size and the strength of the molecule-wall interaction (modeled by Lennard-Jones potential) were related to the thickness of the adsorbed layer on the pore wall (i.e., the quantity adsorbed). This model has been shown to describe the adsorption behavior of Nitrogen in samples of molecular sieve MCM-41 (mesoporous solid) characterized by different pore sizes. However, this approach is not suitable for microporous solids because the small amount of fluid molecules within each micropore would invalidate the theory of interfaces that has been thermodynamically described for macro or mesoscopic systems.

Schoen and Diestler[4] proposed an extension of the van der Waals equation of state for fluids confined in rectangular pores. These authors relied on Perturbation Theory, with reference to a fluid of hard spheres with uniform density. A correction was defined based on the mean-field approximation to account for the attractive effect of the molecule-molecule and molecule-wall (both modeled by Lennard-Jones potential) interactions. The only difference between this equation of state and van der Waals is the

energy parameter, which is a function of the distance between the solid walls for confined fluids. This model was able to qualitatively predict some effects of the confinement in fluids experimentally adsorbed on mesopores, such as capillary condensation and reduction of the critical temperature of the fluid due to the reduction in pore size. However, the model predicts that the critical density of the fluid is independent of pore size, which is a consequence of the assumption of uniform density of the confined fluid. Furthermore, the authors reported that their model does not adequately describe the adsorption under near the critical point of the unconfined fluid. To avoid this problem, molecular simulation results suggest a need to consider various regions inside the pore that are dependent on the distance from the wall. Thus, the properties of fluids under confinement are a result of the contributions of each region, thus allowing a simplified representation of the variation of the fluid density in the radial direction of the pore.

Truskett et al.[5] extended the Diestler and Schoen model[4] so as to consider the occurrence of hydrogen bonds between the molecules of fluid, aiming to describe the associative behavior of fluids (for example: water) under confinement. But Giaya and Thompson[6] observed that the predictions of this model appeared to be very sensitive to the values of some parameters, which could affect the performance of the model. Thus they proposed a change in the method of accounting for the effect of hydrogen bonds on the properties of the fluid. This methodology has been extended to cylindrical pores, obtaining predictive results consistent with experimental observations concerning water adsorption in two mesoporous materials.

Zarragoicoechea and Kuz[7] developed an extension of the van der Waals equation of state to fluids confined in pores with finite areas. These authors began with a classical thermodynamic formulation, together with the premise that the pressure of the confined fluid has tensor character, given the anisotropic nature of the system. The molecule-molecule interaction was modeled by a Lennard-Jones potential and the attractive molecule-wall interaction was neglected. This model was used to predict the conditions of the fluid capillary condensation, and obtained results that were comparable to those provided by network models and numerical simulations.

Derouane[8] proposed a modification of the simple attractive van der Waals equation of state to create an appropriate model to predict the density and physical state of fluid molecules adsorbed in microporous solids at or near pore saturation conditions. A term dependent on the pore radius was added to the original equation of state, which refers to the increase of fluid pressure due to the increase in the degree of confinement, as suggested by experimental study. The repulsive effect of confinement was not altered, due to experimental indications that the van der Waals volume parameter suffers a slight reduction (approximately 15%) for confined fluids. This model was able to qualitatively describe the critical density increase and a decrease in the critical temperature as a result of a reduction of the pore size. Although the repulsive part of the van der Waals equation has not been modified, an approach was suggested by which such a modification could be performed in order to obtain more quantitative predictions suitable for the adsorption of fluids in micro-and mesoporous solids.

Sandler[9] describes that the total energy of such an assembly of molecules can be separated into translational, rotational, vibrational, electronic and interaction energy. Each of these energy contributions is assumed to be independent of each other. The generalized van der Waals equation can be modified to fit several EOS based on the assumptions made for the free volume, V_f and mean potential, φ. Van der Waals developed the expression for free volume based on its literal meaning, i.e. the volume that is available for a new molecule of diameter σ to be introduced into a volume V occupied by N similar molecules. Van der Waals also assumed that the coordination number is a function of density and is independent of temperature. The square well model is chosen due to its simplicity, and because expressions such as the coordination number can be well defined without any ambiguity.

Woods *et al.*[10] investigated the thermodynamic behavior and local density for the adsorption of molecules in zeolites with spherical cavities, with the molecules following Lennard-Jones behavior. The different methods undertaken were a direct calculation of the partition function, a derivation of the results yielded by the expansion of the virial coefficient expression, and use of the grand canonical Monte Carlo simulations as a comparison tool for the former methods. The partition function results were found to be better than those obtained from the virial coefficient expression. These results were then compared to the Monte Carlo simulation. The result for occupancy in the adsorbents was an interesting focal point of this paper. Two adsorbent systems were chosen for study, namely xenon in faujasite (large cavities) and a reduced version of a similar system (small cavities). For both large and small cavities, the average occupancy was 4

molecules per pore, with the actual occupancy ranging from 1-7 molecules. For larger cavities, discrepancies were noted between the partition function calculations and simulation results when the average occupancy was greater than 5. The small cavity results were in agreement for all occupancies.

Travalloni *et al.*[2] extended the generalized van der Waal's equation for confinement in cylindrical pores. The interactions between the fluid molecules, as well as the fluid molecules with the walls were modeled using the square-well theory. This procedure involved developing empirical expressions for the coordination number, porosity and the free volume, which were in turn implemented in the configurational energy equation. Adsorption calculations were then performed to study the performance of this model, as well as its sensitivity to the fitted parameters. This work will employ a similar technique of developing an equation of state, while making necessary modifications for spherical pores.

CHAPTER III

THERMODYNAMIC MODEL

Through use of statistical thermodynamics, the generalized van der Waals approach was adopted as a basis for the development of an equation of state that could model fluids under the effects of confinement in porous media. These models are designed as extensions of simple cubic equations of state, with aspects related to these equations of state included in terms that characterize confinement, i.e., pore size and the strength of the interactions between the fluid molecules and the pore walls. Hence, the modified equation of state obtained is expected to describe the behavior of a fluid as a function of the degree of confinement. This model would apply to the confined fluid, as well as the unconfined fluid, thus providing a simple and consistent adsorption model. To achieve this goal, several hypotheses have been assumed about the adsorbent-adsorbate system, and the resulting models of these hypotheses were obtained analytically through computer algebra. The following is a description of the models whose formulation provided a basis for this work.

According to Hill[11], the properties of a mixture can be obtained from the canonical partition function:

$$Q(T,V,N_1,N_2,\ldots N_{NC}) = \prod_{i=1}^{NC}\left(\frac{q_i^{N_i}}{\lambda_i^{3N_i} N_i!}\right) V_f^N \exp\left(\int_{\infty}^{T}\frac{E_{conf}}{kT^2}\mathrm{d}T\right) \qquad (1)$$

where NC is the number of components, T is the absolute temperature, V is the total volume of the system, N_i is the number of molecules of component i of the fluid, q_i is the

internal partition function for a molecule of component *i*, λ is the de Broglie wavelength (translational energy contribution to the function partition), *k* is the Boltzmann constant, V_f is the free volume and E_{conf} is the configurational energy. For NC=1, equation 1 reduces to the pure component canonical partition function.

The canonical partition function, *Q*, represents a bridge between statistical and classical thermodynamics. Through this expression, various thermodynamic properties such as Helmholtz free energy, *A*, pressure, *P*, and chemical potential of a component *i* can be derived as follows,[9]

$$A(T,V,N_1,N_2...N_{NC}) = -kT\ln Q(T,V,N_1,N_2...N_{NC}) \tag{2}$$

$$P = kT\left(\frac{\partial \ln Q}{\partial V}\right)_{T,N_1,N_2...N_{NC}} \tag{3}$$

$$\mu_i = -kT\left(\frac{\partial(\ln Q)}{\partial N_i}\right)_{T,V,N_{j\neq i}} \tag{4}$$

As per the generalized van der Waals theory, expressions must be defined for the free volume, V_f, which denotes the repulsive part of the equation of state and the configurational energy, E_{conf}, which denotes the attractive part. This is based on the assumption that the fluid molecules are hard spheres that interact with each other through the square-well potential model.

Free Volume Expression

In the case of mixtures, the expression for free volume of the fluid mixture follows,

$$V_f = V - \sum_{i=1}^{NC} \frac{N_i}{\rho_{\max,i}} \tag{5}$$

which, for pure substances, reduces to:

$$V_f = V - N\beta = V - \frac{N}{\rho_{\max}} \tag{6}$$

where β is the excluded volume per fluid molecule and ρ_{max} is the packing density of the fluid. In the case of confined fluids, ρ_{max} is a function of the dimensions of confinement, namely the adsorbent pore size. Applying the assumption of perfectly spherical adsorbent pores with a radius r_p, and fluid molecules are spheres of diameter σ, this leads to ρ_{max} being a function of the r_p/σ ratio. To find out the relationship between these quantities, porosity data is used.

Porosity is a measure of the empty or void spaces in a material. It is the fraction of the volume of void spaces over the total volume, and is normally expressed as a number between 0 and 1. The equation for porosity at packing density follows the same basis as the cylindrical porosity developed by Travalloni *et al.*[2] ρ_{max} is functionally dependent on the mean porosity of loosely packed beds of hard spheres in a spherical pore. In the model, porosity is calculated using the following expression,

$$\xi = c_1 + c_2 \exp\left(c_3\left(0.5 - \frac{r_p}{\sigma}\right)\right) - c_4 \exp\left(c_5\left(0.5 - \frac{r_p}{\sigma}\right)\right) \tag{7}$$

Constants c_1-c_5 were obtained by minimizing the deviation between computer-simulated porosity data results[12] and values calculated using equation 7. These values are displayed in Table 1, while the porosity fit obtained is displayed in Figure 1.

Table 1: Parameters used to calculate porosity

c_1	0.46091
c_2	0.98273
c_3	2.65807
c_4	1.44365
c_5	29.0217

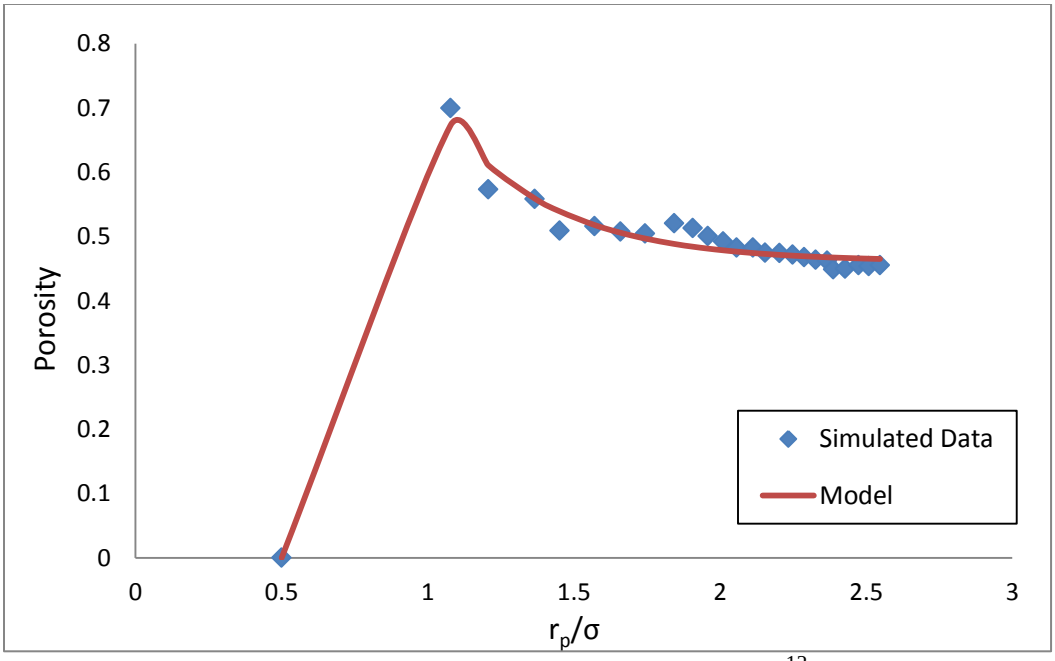

Figure 1: Porosity versus r_p/σ (Pfoertner)[12]

Configurational Energy

The model only considers interactions in regions I and II of the spherical pore, depicted in Figure 2. The first term in the configurational energy expression (equation 8) describes the molecule-molecule interactions taking place in regions I and II of the pore, while the second term explains the molecule-wall interactions that occur in region II of the pore. Interactions in region III are neglected, due to hardcore repulsion from the pore wall, thus rendering this region inaccessible to the mass centers of the fluid molecules.

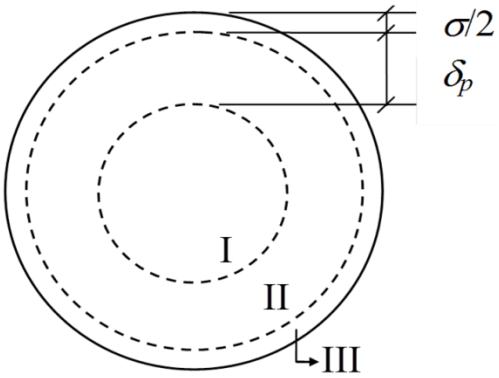

Figure 2: Square-well region inside a spherical pore

The configurational energy describes the interactions between the fluid molecules as well as the interactions between the fluid molecule and the pore wall. From the work by Travalloni *et al.*[2], the configuration energy follows,

$$E_{conf} = -\frac{N}{2} N_C \varepsilon - N F_p \varepsilon_p \tag{8}$$

where N_c is the coordination number, ε is the energy parameter of the molecule-molecule interaction, ε_p is the energy parameter of the molecule-wall interaction and F_p is the fraction of confined fluid molecules that occupy the square-well region of the pores.

Coordination Number and Calculations for Nearest Neighbors

The coordination number is essentially defined as the number of nearest neighbors that a selected particle interacts with[9]. It is necessary to determine the coordination number based on the geometry, as this gives an idea of how the molecules will be distributed within the pore.

Each of the commonly used cubic equation of state, the Peng-Robinson EOS among them, uses a different expression for the bulk coordination number, which needs to be modified to account for the effect of confinement in spherical pores. The formal solution to this problem is to find the radial distribution function of molecules inside the pore. To avoid this difficult calculation and in order to obtain an equation for the coordination number for spherical pores, several empirical functions were investigated, including the generalized logistic function (Richard's curve)[13], the normal distribution function[14] and the sigmoidal function. Out of these, it was determined that a combination of the generalized logistic function[13] and the normal distribution function[14] would provide the best fit to the geometric data[12], i.e. the ratio of the pore size to the molecular diameter, r_p/σ. Hence, the average logistic-normal function was adapted to describe the confinement part of the coordination number. Equation 9 expresses the formula adapted for the confinement coordination number, and equation 10 describes the entire

coordination number. Table 2 displays the fitted parameters and Figure 3 presents its results.

$$W_{ij} = \frac{1}{10}\left[A_n + \frac{K_n - A_n}{\left(1 + Q_n \exp\left(-B_n\left(\left(r_p/\sigma_{ij}\right) - M_n\right)\right)\right)^{\frac{1}{\eta_n}}} - \frac{\exp\left(-\left(\left(r_p/\sigma_{ij}\right) - \mu_n\right)^2 \Big/ 2\sigma_n^2\right)}{\sigma_n\sqrt{2\pi}}\right] \tag{9}$$

$$N_{c,ij} = Wf_{PR,ij}(T)\frac{x_i\rho_{max}}{\sqrt{\rho_{max,i}\rho_{max,j}}}\ln\left(\frac{1+\left(1+\sqrt{2}\right)\rho/\rho_{max}}{1+\left(1-\sqrt{2}\right)\rho/\rho_{max}}\right) \tag{10}$$

Table 2: Average Logistic-Normal Function Constant Values

Parameter	**Value**
A_n	-4.685×10^{-4}
K_n	1.000×10^{1}
Q_n	2.628×10^{-1}
B_n	3.345
M_n	-8.141×10^{-1}
η_n	3.255×10^{-4}
σ_n	2.666×10^{-1}
μ_n	1.794

As in the case of the parameters for porosity (Table 1), the parameters in Table 2 are applicable to any substance or mixture. Thus it is not necessary to refit them during application of the model.

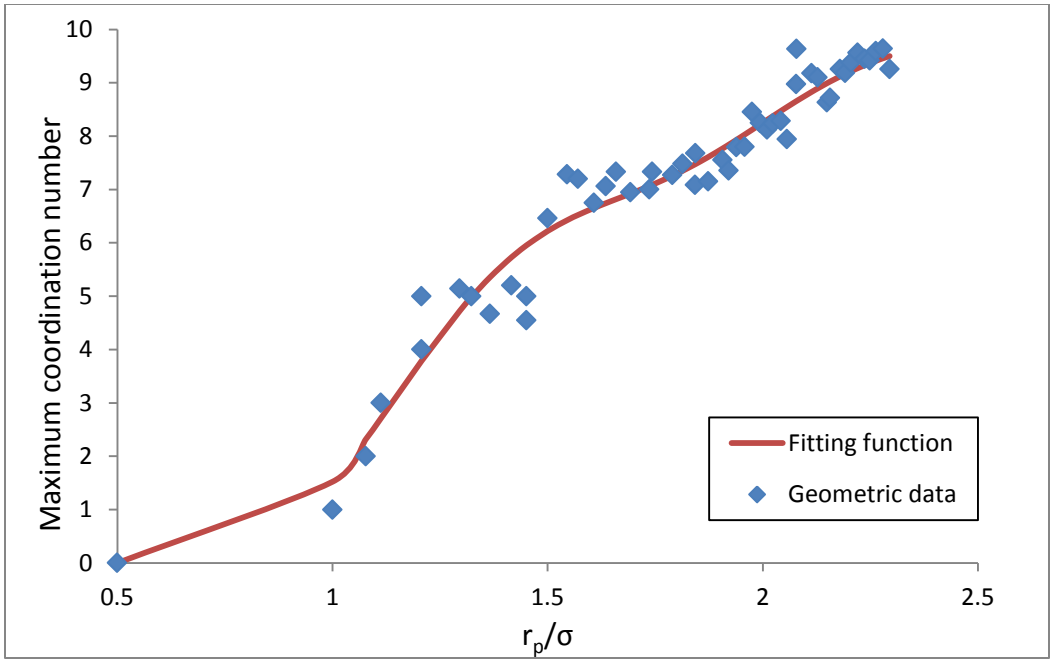

Figure 3: Coordination number versus r_p/σ

The limiting value of N_c as $r_p/\sigma \rightarrow \infty$ in equation 9 is approximately 10. The minimum coordination number is 0, which would result in a configuration of a single sphere confined within a sphere, with no space available for the insertion of additional spheres. Hence the maximum coordination number for a sphere follows the previously observed result for cylindrical pores by Travalloni *et al.*[2], while the minimum coordination number does not follow the previous results.

The best representation of spherical particles confined within a sphere was found on a website entitled *Densest packing of spheres in a sphere*[12]. This website displays 3-D simulations of spheres within a sphere of unit diameter; the URL can be found in the references section. An example of packed spheres inside a spherical cavity is shown in Figure 3. The number of spheres that are to be inserted can be manually adjusted.

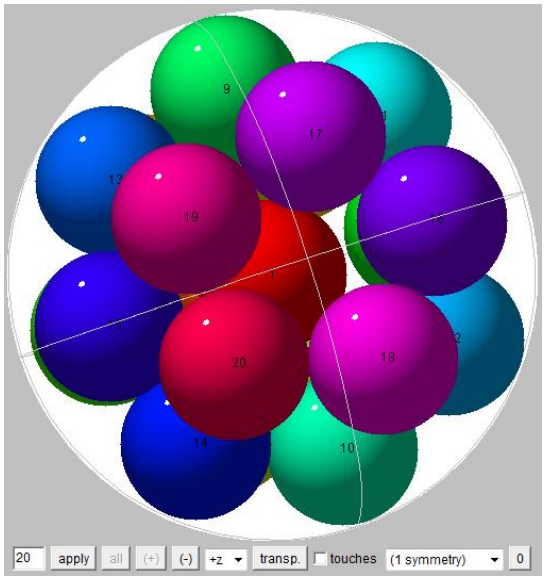

Figure 4: Spherical particles confined within a sphere, n = 20*

In the configurational energy expression, F_p is defined as the fraction of the total number of fluid molecules in region II (the intermediate square-well layer). It is a simplistic way to account for the local distribution of the fluid molecules within each adsorbent pore. As in the case of the coordination number, the formal method of finding the local density distribution within the adsorbent is avoided by taking an empirical approach. F_p depends on F_{pr}, which is the fraction of confined molecules in the square-well region of the pores for random distribution of the fluid. It is based on the volume of the pore, which is spherical.

*Image reprinted with permission from "Densest Packing of Spheres in a Sphere" by Pfoertner, H., 2011, Copyright [2011] by Pfoertner, H.

$$F_{pr} = \frac{V^{II}}{V^{I} + V^{II}} \tag{11}$$

The volume of a sphere simply follows the formula below,

$$V^{I} = \frac{4}{3}\pi R^{I^3} \tag{12}$$

$$V^{II} = \frac{4}{3}\pi R^{II^3} \tag{13}$$

Substituting these expressions into F_{pr},

$$F_{pr} = \frac{R^{II}}{R^{I} + R^{II}} \tag{14}$$

$$F_{pr} = \frac{\left(r_p - \frac{\sigma}{2}\right)^3 - \left(r_p - \frac{\sigma}{2} - \delta_p\right)^3}{\left(r_p - \frac{\sigma}{2}\right)^3} \tag{15}$$

An empirical expression was developed for F_p in order to avoid complications in determining the local distribution of the confined fluid, which follows,

$$F_p = F_{pr} + \left(1 - F_{pr}\right)\left(1 - \exp\left(\frac{-\varepsilon_p}{kT}\right)\right)\left(1 - \frac{\rho}{\rho_{\max}}\right)^{\theta} \tag{16}$$

and satisfies different physical limits of the confined fluid. When $\rho \rightarrow \rho_{max}$ and $T \rightarrow \infty$, $F_p = F_{pr}$, which means that the fluid is randomly distributed in the pores. When $\rho \rightarrow 0$ and $T \rightarrow 0$, $F_p = 1$, and the confined molecules occupy the square-well region of the pores.

θ is a geometric term that defines the relationship between the real and maximum pore radius and accounts for all fluid molecules that are attracted to the pore wall. The

expression for θ can be assumed to follow the same formula as in the case of cylindrical pores i.e.

$$\theta = \frac{r_p}{\delta_{p,i}+\frac{\sigma_i}{2}} \tag{17}$$

Extended Peng-Robinson Equation of State

The expression for the extended Peng-Robinson equation of state developed by Travelloni *et al.*[15] for confined fluids (PR-C) is as follows,

$$P = \frac{RT}{v-b_p} - \frac{a_p(T)}{v\left(v+b_p\right)+b_p\left(v-b_p\right)} - \theta\frac{b_p}{v^2}\left(1-\frac{b_p}{v}\right)^{\theta-1}\left(1-F_{pr}\right)\left(RT\left(1-\exp\left(-\frac{N_{av}\varepsilon_p}{RT}\right)\right)-N_{av}\varepsilon_p\right) \tag{18}$$

where R is the universal gas constant, a_p is the confinement-modified energy parameter of the fluid mixture, b_p is the confinement modified volume parameter, ν is the molar volume of the fluid, F_{pa} is the fraction of confined molecules in the square-well region of the pores for random distribution of the fluid, and θ is the geometric factor.

The development of the model follows the steps of the work of Travelloni *et al.*[15] for confined fluids except for details related to the pore geometry, which is spherical here as opposed to cylindrical in the original publication. The working expressions for a_p, which is the modified energy parameter for confinement of the fluid mixture, and for b_p , which is the modified volume parameter for confinement of the fluid mixture, are:

$$a_p = \sum_{i=1}^{NC}\sum_{j=1}^{NC}\left(x_i x_j a_{p,ij}\right) \tag{19}$$

$$b_p = \sum_{i=1}^{NC} x_i b_{p,i} \tag{20}$$

The auxiliary terms to evaluate a_p are expanded as follows:

$$a_{p,ij} = W_{ij}\sqrt{a_i a_j}\left(1-k_{ij}\right) \tag{21}$$

$$W_{ij} = \frac{1}{10}\left[A_n + \frac{K_n - A_n}{\left(1+Q_n \exp\left(-B_n\left(\left(r_p/\sigma_{ij}\right)-M_n\right)\right)\right)^{\frac{1}{\eta_n}}} - \frac{\exp\left(-\left(\left(r_p/\sigma_{ij}\right)-\mu_n\right)^2/2\sigma_n^2\right)}{\sigma_n\sqrt{2\pi}}\right] \tag{22}$$

The parameters of equation 21 are presented in Table 2. Additional intermediate terms are:

$$\sigma_{ij} = \frac{\sigma_i + \sigma_j}{2} \tag{23}$$

$$\sigma_i = \sqrt[3]{\frac{1.029581 b_i}{N_{av}}} \tag{24}$$

$$\mathrm{b}_i = \frac{0.0778 R T_{ci}}{P_{ci}} \tag{25}$$

$$a_i = \frac{0.45724 R^2 T_{ci}^2\left(f_{w,i}\left(1-\sqrt{\frac{T}{T_{ci}}}\right)+1\right)^2}{P_{ci}} \tag{26}$$

$$\mathrm{f}_{wi} = 0.37464 + 1.54226\omega_i - 0.26992\omega_i^2 \tag{27}$$

The auxiliary terms to evaluate b_p are expanded as indicated here. First, $b_{p,i}$ is the confinement modified volume parameter of pure component *i*,

$$b_{p,i} = \frac{N_{av}}{\rho_{\max,i}} = \frac{1}{\rho_{n,\max,i}} \tag{28}$$

where $\rho_{max,i}$ and $\rho_{n,max,i}$ are the number packing density and molar packing density of pure component i, respectively, and N_{av} is the Avogadro number. $\rho_{n,max,i}$ depends on the molecule size, as well as the pore size as follows:

$$\rho_{n,\max,i} = \frac{1.02958 - 1.87689e^{2.65807\left(0.5-\frac{r_p}{\sigma_i}\right)} + 2.75716e^{29.0217\left(0.5-\frac{r_p}{\sigma_i}\right)}}{\sigma_i^3 N_{av}} \tag{29}$$

where σ_i is given by equation 23 and b_i, upon which it depends, is given by equation 24.

Comments

It should be remarked that the model presented in this chapter is developed to represent the behavior of many molecules in many pores. It is not intended for the individual modeling of a single pore.

Another interesting detail about the development of a model for fluids in a spherical pore is how to obtain volume derivatives, such as that of the Helmholtz function, which gives the formula for pressure. There are many ways of changing the volume of pore space in a medium. In this discussion, two are considered. The first is to change pore diameter, keeping the number of pores constant. The second is to change the number of pores while maintaining constant diameter.

When dealing with bulk fluids, any changes in volume would not have a major effect on how the molecules interact with the confining wall (as this effect, on average, is negligibly small). Therefore, volume changes affect the space available for the molecules without affecting the characteristics of their interaction with the confining wall. For confined fluids, the pressure in the pore was computed in analogous fashion,

i.e., the volume was modified in a virtual process that changes the number of pores but maintains constant diameter.

CHAPTER IV

ZEOLITES

In order to compare the calculated and experimental adsorption results, it is necessary to determine which porous materials would be suitable for this purpose. Through use of the Dortmund Data Bank[16], ZEOMICS[17] and published papers, a list of zeolites which have near spherical structures were identified and compiled, as per Table 3. Zeolites have been used for the purpose of adsorption and catalysis for the past 50 years. Due to their regular cavity shape and size, zeolites prove to be suitable candidates for studying the effects of confinement.

The adsorbents considered for analysis were mainly zeolite A, which follows the LTA structure[17], sodalite, which follows the SOD structure[17] and chabazite, which follows the SSZ-13 structure[17]. The reason for the selection for these zeolites is the vast amount of adsorption data available from literature. All three zeolites have nearly spherical pores, with some cylindrical structures acting as connectors or channels to the spherical pores. For simplicity's sake, the effect of the cylinder is assumed to be negligible, i.e. the zeolites are assumed to be purely spherical.

This work focuses on the adsorption of methane, ethane, propane, and butane, which are abundant in Qatar as some of the major components of natural gas. Both pure component and binary mixture literature data were compiled.

Table 3: Spherical Zeolite Classification

Structure	Name
ASV	ASU-7
ATN	MAPO-39
DDR	Deca-dodecasile 3R
DFT	DAF-2
LTL	Linde Type L, zeolite L
MEP	Melanophlogite
MOZ	ZSM-10
OSO	OSB-1
RTE	RUB-3
RTH	RUB-13
RWY	UCR-20
SAS	STA-6
SFF	SSZ-44
SOD	Sodalite
SSZ-13	Chabazite
TSC	Tschortnerite
UOZ	IM-10
LTA	Zeolite A
-	Zeolite 13X

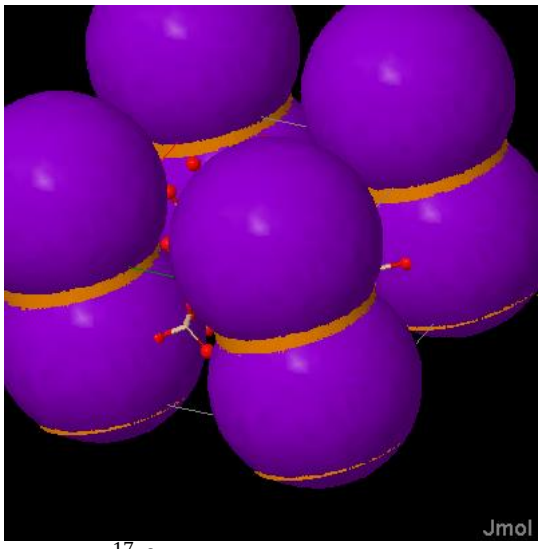

Figure 5: Zeolite A[17] follows the Linde type A (LTA) structure[†]

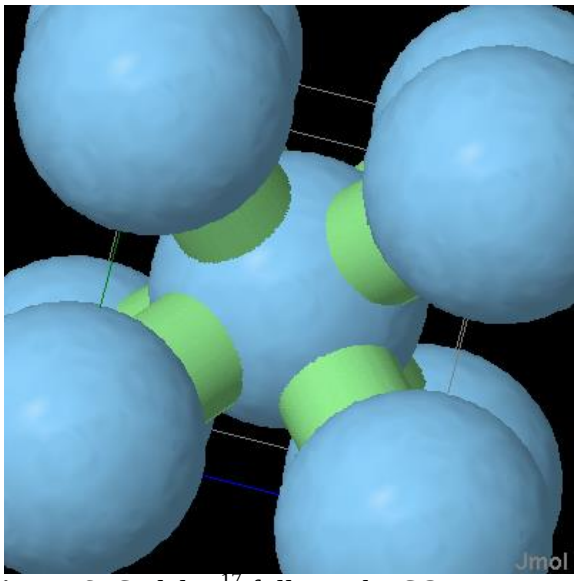

Figure 6: Sodalite[17] follows the SOD structure[†]

[†]Zeolite images reprinted with permission from "ZEOMICS - Zeolites and Microporous Structures Characterization" by First, E. L., and Floudas, C. A., 2011., Copyright [2011] by Floudas, C. A.

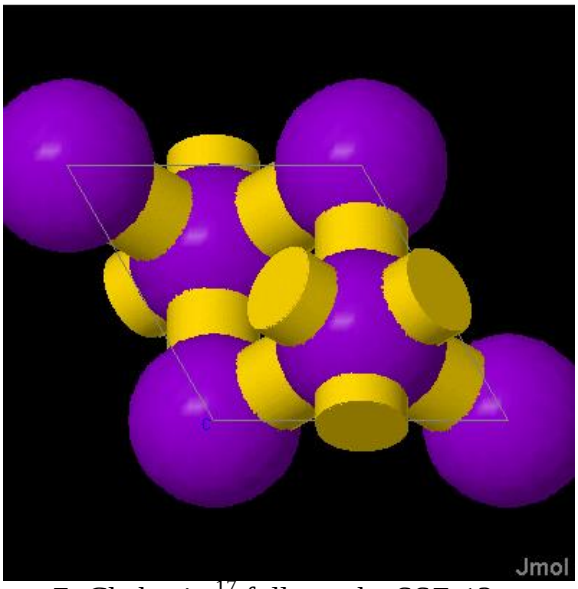

Figure 7: Chabazite[17] follows the SSZ-13 structure[†]

Table 4 details the structural properties of the adsorbents considered. This table includes information about the largest cavity diameter, which is an important quantitative characteristic of the pore, as well as the specific pore volume, which is the sum of all the pore volumes per one gram of adsorbent. The sodalite structured zeolites considered are ZIF-8, ZIF-90, ZIF-Cl, ZIF-NO_2, and ZIF-COOH.

Table 4: Zeolite properties

Adsorbent	**Largest Cavity Diameter (m)**	**Specific Pore Volume (m^3/kg)**
Chabazite	8.75×10^{-10}	3.21×10^{-4}
Deca-dodecasile 3R	8.75×10^{-10}	3.21×10^{-4}
Zeolite 13X	1.30×10^{-9}	3.60×10^{-4}
Zeolite A	1.11×10^{-9}	5.08×10^{-4}
Zeolite L	1.72×10^{-9}	4.30×10^{-4}
ZIF-8 (sodalite)	1.16×10^{-9}	5.20×10^{-4}
ZIF-90 (sodalite)	1.72×10^{-9}	4.30×10^{-4}
ZIF-Cl (sodalite)	1.70×10^{-9}	4.10×10^{-4}
ZIF-COOH (sodalite)	1.72×10^{-9}	4.30×10^{-4}
ZIF-NO_2 (sodalite)	1.71×10^{-9}	4.00×10^{-4}

CHAPTER V

EQUILIBRIUM CALCULATION AND PARAMETER FITTING

Parameter Fitting

The formulas for coordination number, porosity and free volume were inserted into the canonical partition function of the extended Peng-Robinson model. Using relationships of classical thermodynamics, it is possible to obtain expressions for pressure, component fugacities and other thermodynamic properties. The Thermath[18] computer algebra package, which is based on Mathematica, was used for this purpose, generating code in Visual Basic, then inserted in the XSEOS[19] package. The goal of these calculations is to determine the confined phase properties, such as pressure and adsorbed amount. The entire numerical process is carried out in the XSEOS[19] spreadsheet, by using functions that have been programmed into the spreadsheet and modifying existing functions through Visual Basic code.

Visual Basic is used to modify and create functions that will be required for the calculations, such as *prslnphiV* ($\ln \Phi_v$) and *prsvv*, which are the values in the vapor phase of the natural logarithm of the fugacity coefficient and molar volume, respectively. The arguments required for these functions are the universal gas constant, pressure, temperature, mole fraction, and the properties of the substance such as critical temperature T_c, critical pressure P_c, acentric factor ω and the binary interaction parameter k_{ij} (zero for pure components). The spreadsheet is divided into four sections,

namely experimental adsorption data, unconfined phase or bulk phase properties, confined phase properties and equilibrium conditions.

Pure Components

For pure substances, it is important to obtain characteristic properties of the confined phase such as the energy parameter ε_p, the size parameter δ_p/σ, and the pressure. In order to calculate these properties, equilibrium conditions are implemented by assuming that the fugacities in the bulk and confined phases are equal, noting that the pressures in the bulk phase and confined phase are different. The aforementioned characteristic properties are attained by using Excel's Solver function to minimize the squared relative deviation (objective function) between the experimental and calculated adsorbed amounts.

The molar volume is then calculated using the *prsvv* function built into XSEOS[19], and the inverse yields the molar density. Finally, the calculated adsorbed amount values are obtained by multiplying the molar density and the specific pore volume of the adsorbent. The adsorption isotherm is then plotted using the calculated adsorbed amount versus the bulk phase pressure.

The steps are summarized as follows,

1. Obtain experimental data for isothermal adsorption components, namely the adsorbed amount and bulk phase pressure, as well as the adsorbent information such as pore radius and specific pore volume.

2. Perform calculations for the fugacity in the bulk phase, using the extended Peng-Robinson equation of state for confined fluids, assuming an infinitely large pore size, and assigning a value of zero to the size and energy interaction parameters.

3. Assign initial estimates for the size and energy parameters in the confined phase.

4. Perform calculations for the fugacity of the confined phase, using the extended Peng-Robinson equation of state for confined fluids, by implementing the specified pore radius as well as the size and energy interaction parameters.

5. Calculate the molar volume by using the *prsvv* function built into XSEOS[19]. The inverse yields the molar density. The calculated adsorbed amount values are obtained by multiplying the molar density and the specific pore volume of the adsorbent.

6. Using Solver, minimize the sum of the squared differences between calculated and experimental adsorbed amounts by changing the characteristic size and energy parameters and adsorbed phase pressure. The bulk and confined phase fugacities are assumed to be equal, i.e. the isofugacity conditions are constraints in the minimization.

7. Plot the adsorption isotherm, using the calculated adsorbed amount versus the pressure.

Binary Mixtures

The binary mixture spreadsheet is divided into four sections just like the pure component spreadsheet. The energy parameter $\varepsilon_{pi,j}$ and the size parameter $\delta_{pi,j}$ values are not calculated but are obtained from the respective pure component files. It is also necessary to know the characteristic properties of the components, which include T_c, P_c, ω and k_{ij}. In the case of this model, the value for k_{ij} is not obtained from literature but is calculated in order to give more accurate results. This value is reported as the scaled k_{ij} in the spreadsheet.

For binary mixtures, the aim is to obtain the characteristic properties of the confined phase by minimizing the total relative deviation squared (objective function) between the experimental and calculated adsorbed amounts. Once these values are obtained, then the experimental and calculated selectivity values are calculated. The calculated adsorbed amount for each component is then calculated by multiplying the molar density, the mole fraction of the respective component and the specific pore volume of the adsorbent. The total adsorbed amount is simply the summation of the adsorbed amounts of the components. Finally, the binary mixture adsorption isotherm is plotted by using the calculated adsorbed amounts versus the bulk phase pressure.

In the case of binary systems, it is beneficial to obtain pure component data from the same source as the mixture data, as the experimental conditions will be very similar. This would lead to consistent pure component results, which will provide a basis for estimation of the mixture parameters. Inconsistencies in the experimental data lead to incorrect model predictions.

XSEOS Spreadsheet Calculations

The XSEOS[19] spreadsheet used for adsorption calculations depends on the Visual Basic code that runs in the background. The code includes definitions for thermodynamic properties related to cubic equations of state, which in this case is mainly the Peng-Robinson equation of state that has been modified for confinement in spherical pores. These thermodynamic functions are evaluated through Visual Basic functions, many of which need specified values of pressure, temperature and mole fractions. As usual with equations of state, it is thus necessary to find the molar volume before evaluating other properties.

The Topliss *et al.*[20] technique is the standard root-finding method used in the XSEOS[19] spreadsheet to evaluate equations of state. This technique is suitable to determine the roots of cubic equations of state and non-cubic equations of state that have three roots in the region of possible physical interest. However, Travalloni *et al.*[15] discovered that the Peng-Robinson equation of state extended to cylindrical pores may have up to five roots in the region of physical interest. In this particular case, the Topliss *et al.*[20] technique is not applicable. Therefore, Travalloni *et al.*[2] used a brute force approach to root-finding that brackets the roots by scanning possible density values, from near-zero to the packing density. No similar study about the number of roots of the Peng-Robinson equation of state extended to spherical pores was conducted. As a precautionary measure, the brute force equation of state root-finding method was employed.

CHAPTER VI

RESULTS AND DISCUSSION

Results based on the new equation of state are presented in this chapter. The comparison of the calculated results versus experimental data was represented through the use of adsorption isotherms, by plotting adsorbed amount versus bulk phase pressure. The results were obtained by minimizing the objective function, i.e. the squared relative deviation between the experimental and calculated adsorbed amount data.

This chapter represents plots of pure component adsorption, accompanied by plots of the mixtures. For mixtures, the fitted parameter values, i.e. ε_p and δ/σ, were simply extracted from the solved pure component files.

Zeolite A Results

Pure Components

The largest cavity diameter for Zeolite A, obtained from the ZEOMICS[17] website, is 11.7 Å. A summary of the results obtained for pure components adsorbed in zeolite A is displayed in Table 5. These include the number of experimental points (N_{exp}), temperature and pressure range, the value of the fitted parameters (δ/σ and ε_p), the average relative deviation (ARD) and the reference. The overall bulk pressure for these cases never exceeded 5.06 MPa, hence there was no opportunity to observe the behavior of the model at very high pressures, only at low and moderate pressures.

For the hydrocarbons in Table 5, there is an increase in the energy parameter (ε_p) with the addition of each CH_2 group. However, there is no clear trend for the size parameter (δ_p/σ). The average relative deviation (ARD) has been calculated for all the data, with the largest relative deviations often occurring at low bulk phase pressures.

The pure component methane fit[21] in Figure 8 shows an underestimation of the calculated amount at lower pressures, and an overestimation of the amount at higher bulk phase pressures, which go up to 5 MPa, with an ARD of 10.58%. The methane[22] plot in Figure 9 has a good qualitative fit and smaller ARD value (5.57%), but the experimental bulk phase pressure only reaches about 1.76 MPa. It is interesting to observance the discrepancy of these two experimental data sets, measured at very similar temperatures for the same substance and adsorbent. For example, according to the Sievers[21] data at 303.15 K, the adsorbed amount is 2.666 mol/kg when the bulk phase pressure is equal to 1.167 MPa. According to the Loughlin *et al.*[22] data at 300.15 K, a similar adsorbed amount (2.651 mol/kg) occurs when the bulk phase pressure is equal to 1.76 MPa. There is a difference of about 40% in experimental pressure between these data points, taken from different sources at very similar conditions.

The ethane fitting[23] in Figure 10, with an ARD of 5.89%, is based on a data set that reaches a maximum bulk phase pressure of about 0.08 MPa, i.e., below atmospheric pressure. The plot shows a tendency to underestimate the adsorbed amount at low pressures and overestimate in the upper pressure range.

Table 5: Zeolite A Pure Component Results

Component	N_{exp}	Experimental T (K)	Experimental P range (MPa)	δ_p/σ	ε_p (K)	Reference	ARD (%)
Carbon dioxide	30	303.15	2.0×10^{-4} – 5.06	0.1009	3753.72	Sievers[21]	11.82
Methane	18	300.15	3.5×10^{-2} - 1.76	0.1232	1274.45	Loughlin *et al.*[22]	5.57
	21	303.15	2.51×10^{-4} - 5.05	0.1326	1319.54	Sievers[21]	10.58
Ethane	16	308.15	2.27×10^{-5} – 8.00×10^{-2}	0.2249	2080.50	Glessner and Myers[23]	5.89
Propane	12	300.15	5.5×10^{-4} - 3.50×10^{-1}	0.0923	3088.20	Loughlin *et al.*[22]	20.90
	13	323.15	2.5×10^{-3} - 9.90×10^{-2}	0.0757	3269.62	Grande and Gigola[24]	0.78
	14	423.15	2.6×10^{-3} - 9.90×10^{-2}	0.1428	2173.24	Grande and Gigola[24]	3.24
n-butane	15	308.15	3.3×10^{-5} – 8.00×10^{-2}	0.1286	4294.34	Glessner and Myers[23]	20.81

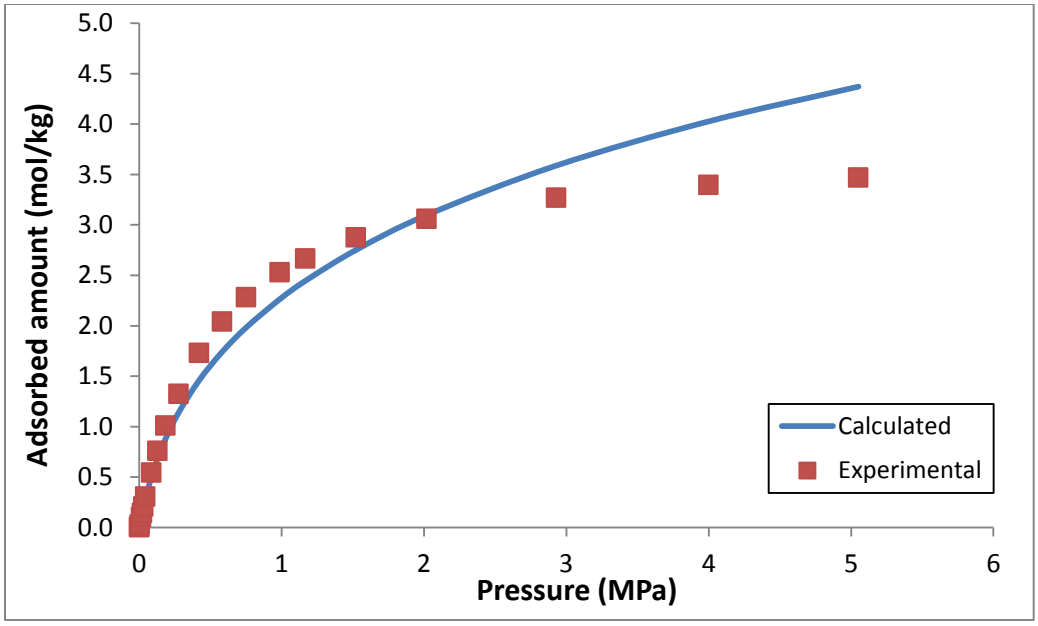

Figure 8: Calculated versus experimental results for methane adsorbed in zeolite A at 303.15 K (Sievers)[21]

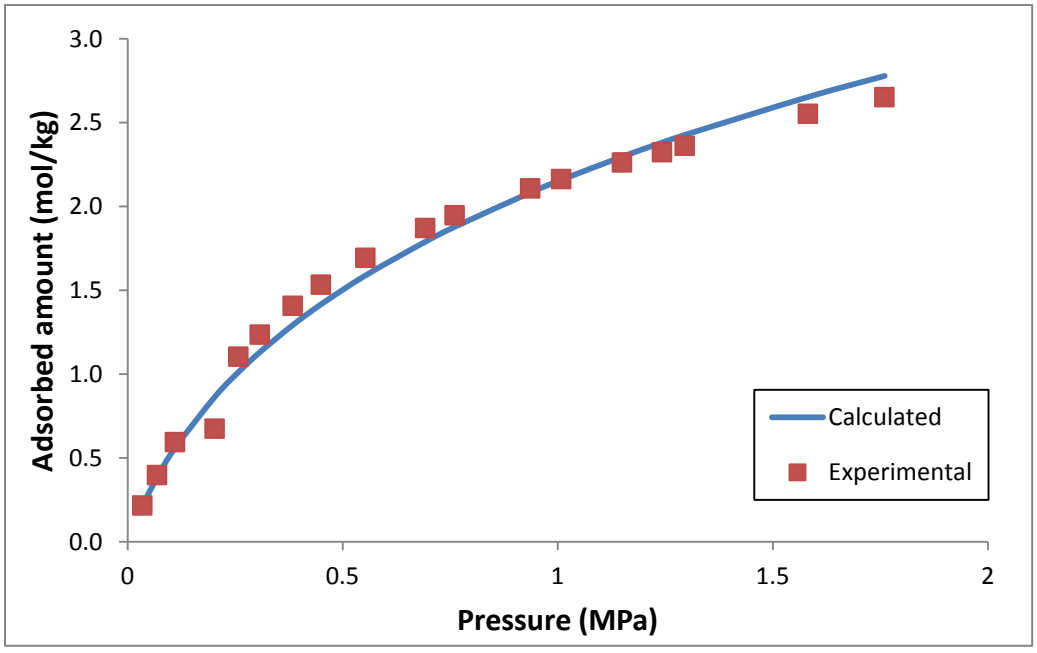

Figure 9: Calculated versus experimental results for methane adsorbed in zeolite A at 300.15 K (Loughlin *et al.*)[22]

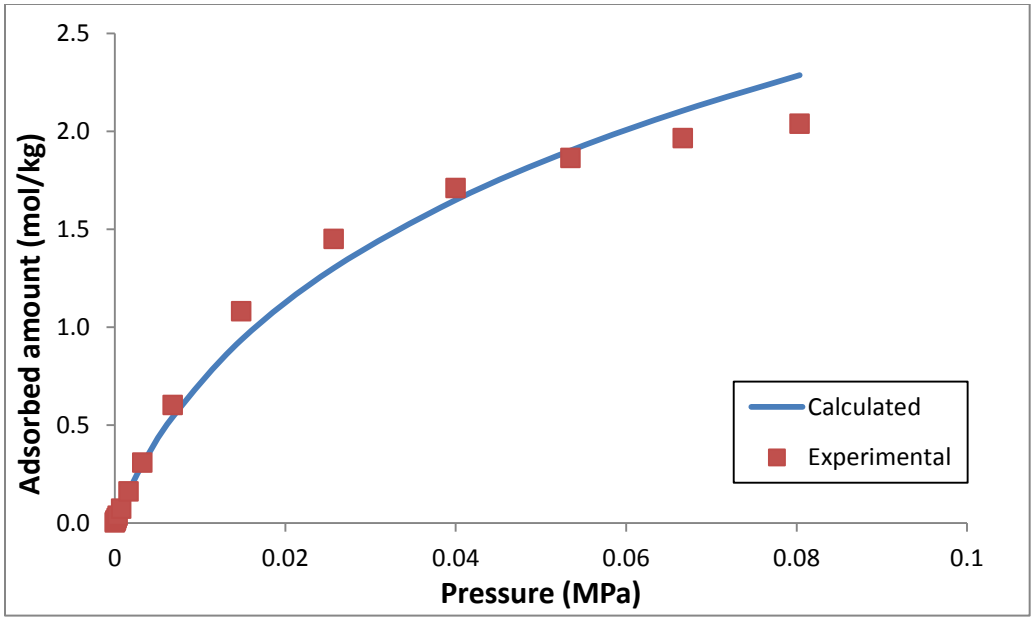

Figure 10: Calculated versus experimental results for ethane adsorbed in zeolite A at 308.15 K (Glessner and Myers)[23]

Temperature dependence on the model was another trend considered. In order to assess the effect of temperature on the model results, adsorption data at different temperatures were analyzed. Propane was the studied component and the adsorption data was modeled at three different temperatures, namely 300.15 K, 323.15 K and 423.15 K. This example again illustrates the discrepancies between experimental data points from different sources. According to the Loughlin *et al.*[22] data at 300.15 K, when the bulk phase pressure is equal to 0.0857 MPa, the adsorbed amount is 1.815 mol/kg. The data of Grande and Gigola[24] at 323.15 K register an adsorbed amount of 2.25 mol/kg for a bulk phase pressure of 0.8041 MPa. Despite being at a lower temperature and higher pressure (conditions that favor adsorption), the value of Loughlin *et al.*[22] is about 20% smaller than the value of Grande and Gigola[24]. The ARD with respect to Loughlin *et*

al.[22] data is 20.9%, with pronounced systematic deviations. However, there is much better agreement with the data of Grande and Gigola[24], with ARDs equal to 0.78% and 3.24%, at 323.15 K and 423.15 K, respectively. The experimental data show that temperature has a sizeable effect on adsorbed amounts and the model, fitted with parameters specific to each temperature, was capable of correlating this effect.

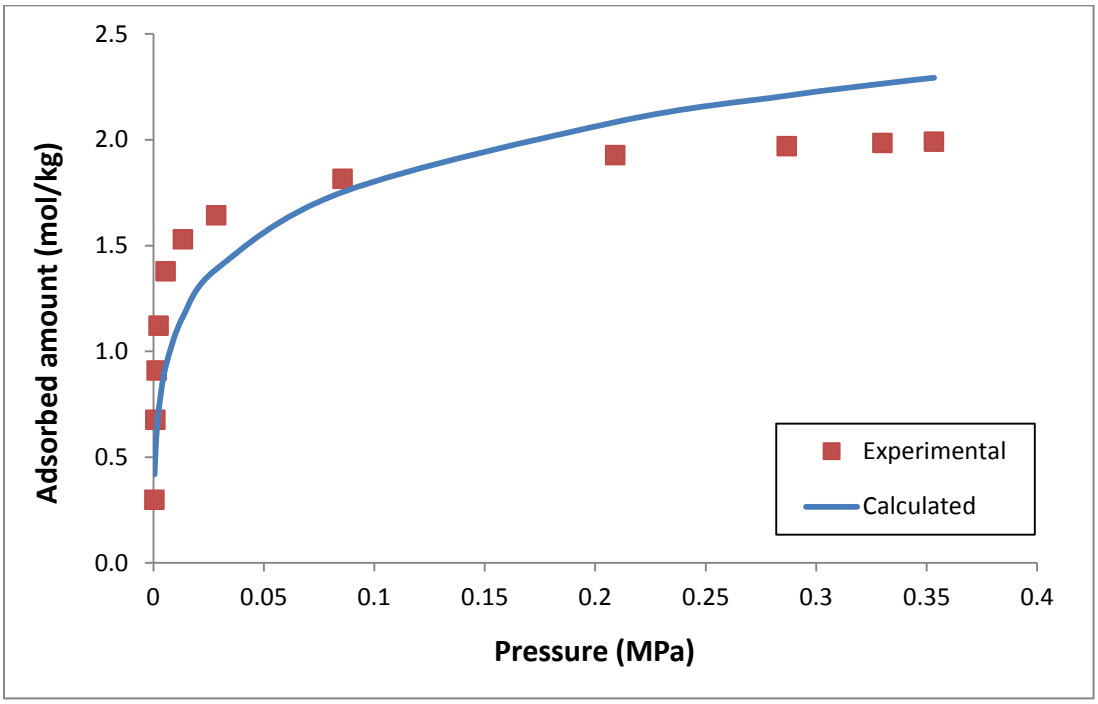

Figure 11: Calculated versus experimental results for n-propane adsorbed in zeolite A at 300.15 K (Loughlin *et al.*)[22]

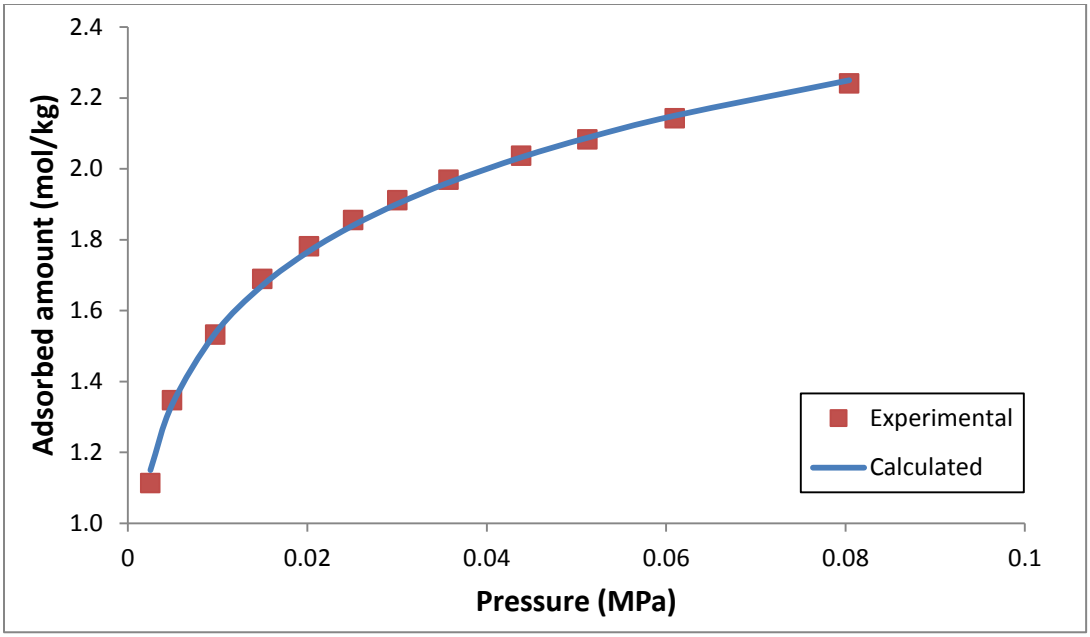

Figure 12: Calculated versus experimental results for n-propane adsorbed in zeolite A at 323.15 K (Grande and Gigola)[24]

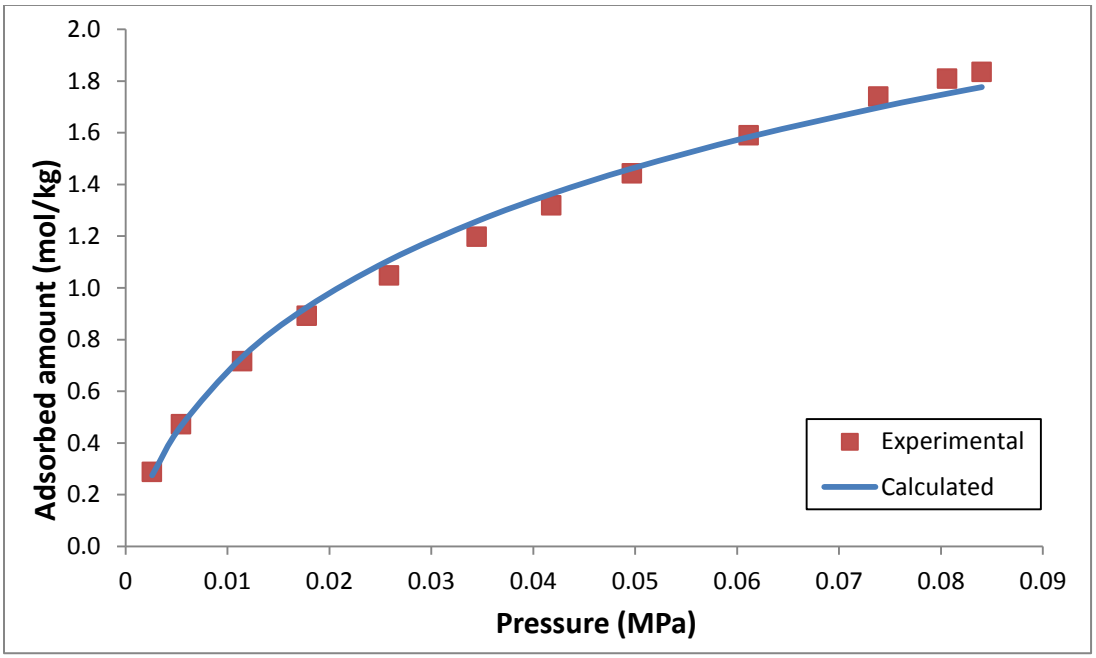

Figure 13: Calculated versus experimental results for n-propane adsorbed in zeolite A at 423.15 K (Grande and Gigola)[24]

The pure component plots for n-butane[23] and carbon dioxide[21] in zeolite A are displayed in Figures 14 and 15, respectively. As in some of the prior cases, the model over predicts the adsorbed amount at what seems to be the pore saturation condition, at the highest bulk phase pressures available from experimental data. Since this phenomenon occurs for the highest amounts within the pore, a possible explanation is that the repulsive part of the equation of state, which is a direct consequence of van der Waals' excluded volume expressions, overestimates the bulk phase pressure and density.

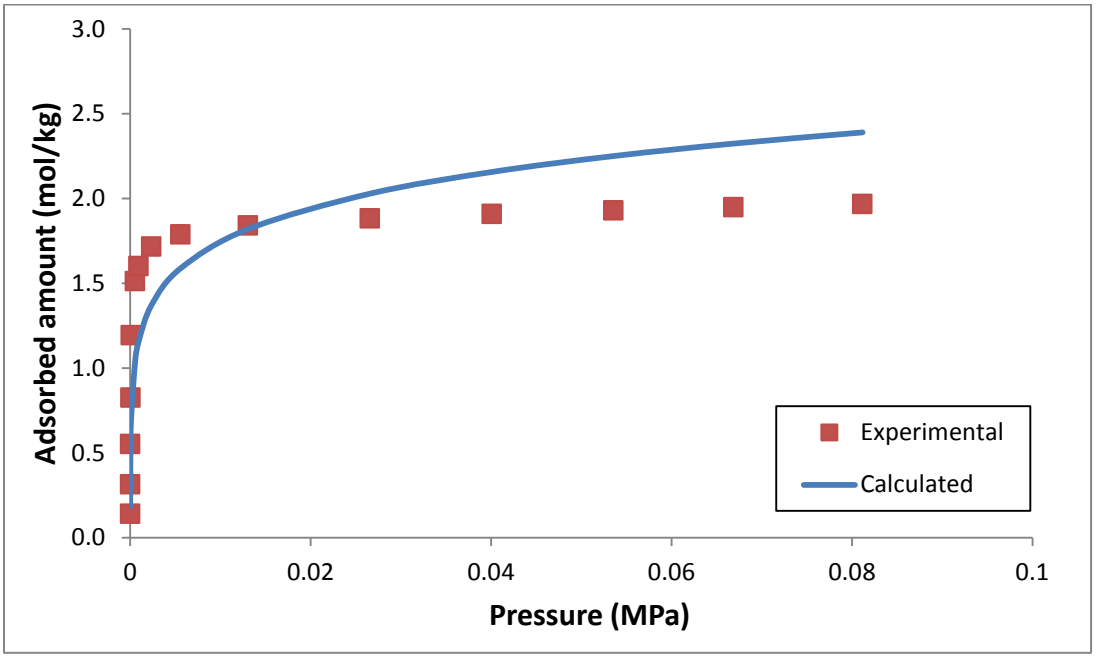

Figure 14: Calculated versus experimental results for n-butane adsorbed in zeolite A at 308.15 K (Glessner and Myers)[23]

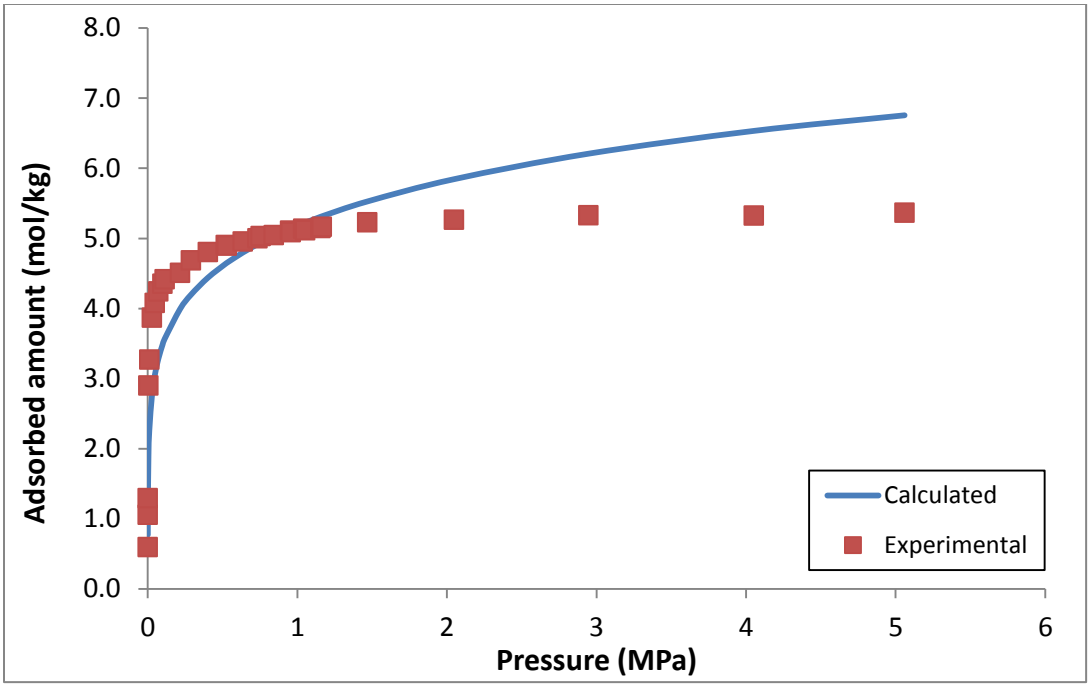

Figure 15: Calculated versus experimental results for carbon dioxide adsorbed in zeolite A at 303.15 K (Sievers)[21]

The average number of molecules inside each pore (average occupancy) was calculated for these systems, each of them at its highest bulk phase pressure, as the product of the fluid density in the pore by the pore volume, and by Avogadro's number. The actual occupancy was then calculated by determining the number of moles (total pore volume divided by molar volume) and multiplying that by Avogadro's number. The calculated occupancy at the highest bulk phase pressure was then compared to the maximum theoretical occupancy. The latter was evaluated based on geometrical considerations, assuming the molecules are spheres (whose effective diameters are listed in Table 6) which are confined inside a spherical zeolite A cavity (diameter, φ = 11.7 Å). This value is used to compute the ratio of the molecule and cavity diameters.

For example, the diameter ratio is equal to 0.3415 for carbon dioxide. A spherical cavity can accommodate 12 spheres with a diameter ratio equal to 0.3445. However, if an attempt was made to fit 13 spheres, their diameter ratio would have to be smaller than 0.3415. Thus, according to these calculations, 12 molecules would be the maximum theoretical occupancy for carbon dioxide in a zeolite A cavity of 11.7 Å diameter. The calculated average occupancy never exceeded the theoretically determined value. Table 6 displays all the theoretical and calculated occupancy numbers for each component in zeolite A.

Table 6: Occupancy number calculations for pure components in Zeolite A

Component	**Molecular Diameter, d (Å)[25]**	**Calculated Diameter Ratio (d/φ)**	**Theoretical Diameter Ratio**	**Maximum Theoretical Occupancy**	**Average Calculated Occupancy, N**
Carbon dioxide[21]	3.99	0.3415	0.3445	12	6.72
Methane [21]	3.78	0.3231	0.3235	14	4.35
Methane[22]	3.78	0.3231	0.3235	14	2.76
Ethane[23]	4.39	0.3750	0.3780	8	2.27
Propane[22]	4.93	0.4217	0.4494	4	2.28
n-Butane[23]	5.60	0.4790	0.4641	3	2.38

Mixtures

Figure 16 shows the results for the adsorption of mixture of methane and carbon-dioxide adsorbed in zeolite A at 303.15 K. The experimental bulk phase pressure of each experimental data point is different, ranging from to 3.086 to 3.168 MPa. The fitted pure component parameters of methane and carbon dioxide (Table 5, Figures 8 and 15) were used. Calculations under the assumption that the cross binary interaction parameter follows $k_{12}=k_{21}=0$ failed to produce acceptable results for this mixture. Thus, the binary interaction parameter k_{12} ($=k_{21}$) was estimated using the binary mixture data. In the use of conventional cubic equations of state, the generally expected range for a k_{ij} parameter is between 0 and 1. Treating it as an entirely empirical parameter, its value was found to be equal to 3.95, and this is possibly due to the effect of confinement. Given the complexity of the modeled situation and the limited experience with this new thermodynamic model, it is difficult to pinpoint the exact reason for this large value of the binary interaction parameter. It may be an issue with the mixing rules or a consequence of deficiencies in other parts of the model. Despite these underlying concerns, this plot shows a good adherence of the calculated values to the experimental trends.

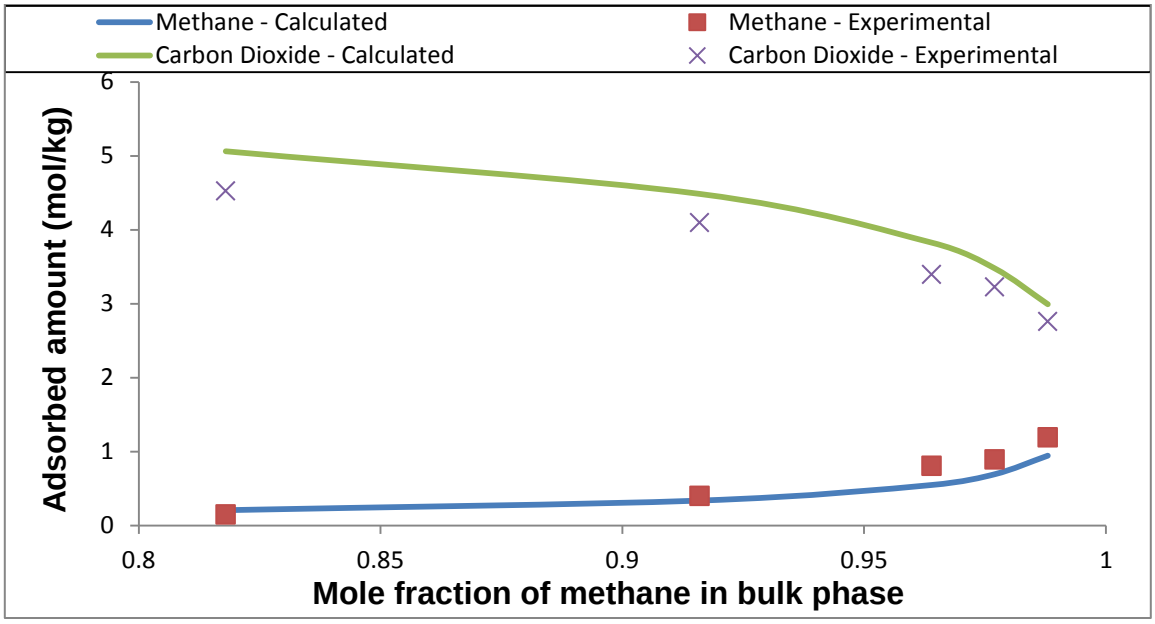

Figure 16: Calculated versus experimental results for a mixture of methane and carbon-dioxide adsorbed in zeolite A at 303.15 K and about 3.1 MPa, fitted k_{ij} value of 3.95 (Sievers)[21]

Figure 17 displays results for a binary mixture of ethane and n-butane using the available pure component parameters (Table 5, Figures 10 and 14) and a fitted value of the cross binary interaction parameter follows k_{12} (=k_{21}), found to be 1.8. Each experimental data point is at a different bulk phase pressure in the range from 6.38 kPa to 6.60 kPa. The representation here is again related to the adsorbed amount versus the mole fraction of one of the components (ethane) in the bulk phase. This experimental data set poses a very difficult challenge to the model. For a mole fraction of ethane equal to 0.998 in the bulk phase, i.e., almost pure ethane, the adsorbed amount of n-butane is about 2.6 times the adsorbed amount of ethane, and the model is incapable of correlating

this trend. However, as the original reference[23] points out, the uncertainty in the bulk phase mole fractions is very high because of the experimental procedure.

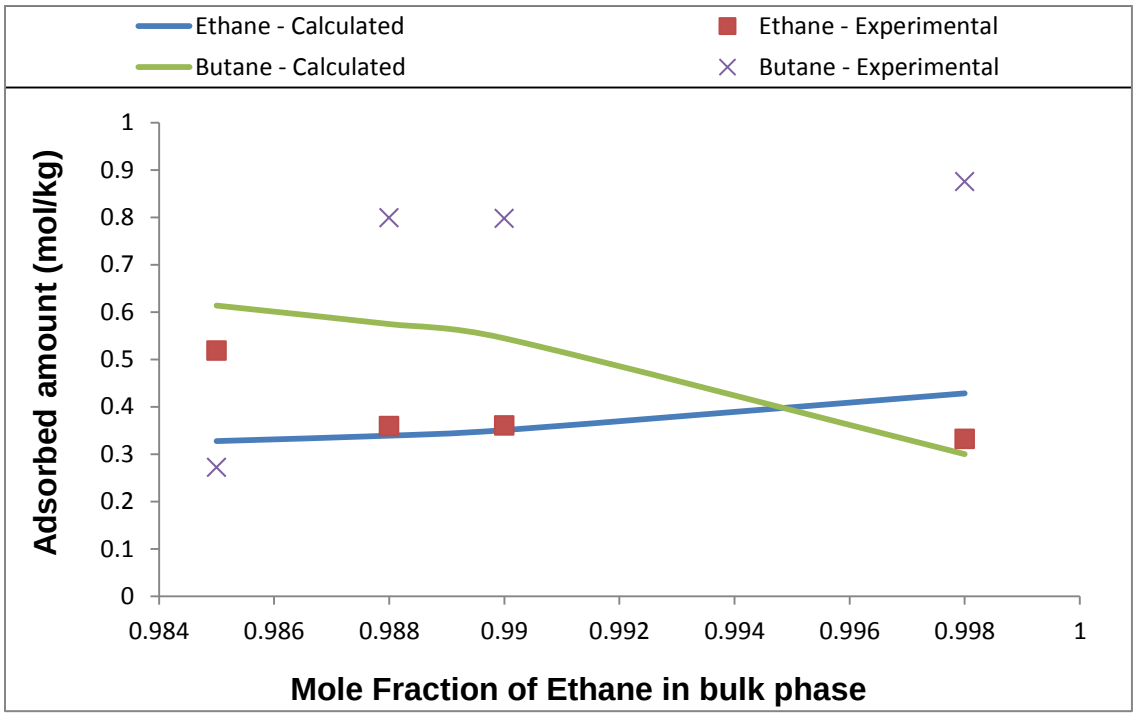

Figure 17: Calculated versus experimental results for a mixture of ethane and n-butane adsorbed in zeolite A at 308.15 K and about 6.42 x 10^{-2} MPa, fitted k_{ij} value of 1.8 (Glessner and Myers)[23]

To attenuate the effect of this uncertainty, the mole fractions in the adsorbed phase were assumed to be fixed and equal to their experimental values. Then, when minimizing the deviations between experimental and calculated adsorbed amounts, the unknowns were the value of k_{12} ($=k_{21}$), the confined phase pressures, and the mole fractions in the bulk phase. This minimization problem is subject to equality constraints, which are the phase equilibrium equations at each experimental condition. The fitted

binary interaction parameter is equal to 1.2. Overall, the reconfigured mixture fit in Figure 18 appears to have improved qualitatively in comparison to the original fitting in Figure 17. The adsorbed amounts have been plotted versus the confined phase mole fraction of ethane as in the original reference[23].

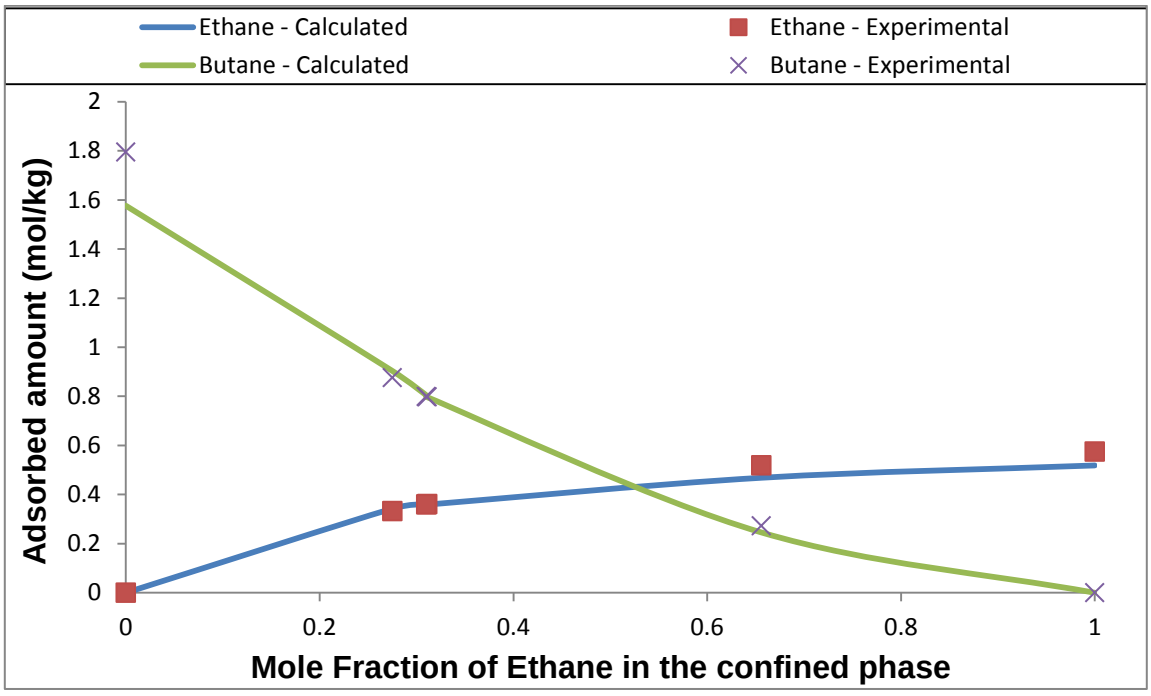

Figure 18: Calculated versus experimental results for a mixture of ethane and n-butane adsorbed in zeolite A at 308.15 K and about 6.42 x 10^{-2} MPa, fitted k_{ij} value of 1.2 (Glessner and Myers)[23]

Sodalite Results

Pure Components

The adsorption of methane and carbon dioxide in a sodalite type adsorbent, ZIF-8, was also studied, and the results of these fits are displayed in Table 7. The diameter of the ZIF-8 adsorbent pores is slightly smaller than zeolite A, at 11.6 Å, and this value was obtained from the work by Nieto-Draghi *et al*[26]. The ARDs for methane and carbon dioxide are equal to 8.56% and 9.03%, and the deviations at the highest bulk phase pressure of each respective plot are equal to 8.2% and 18.9%. The average pure component occupancy numbers at the highest bulk phase pressure are found to be 8.63 molecules for methane and 4.97 molecules for carbon dioxide.

Table 7: Sodalite Pure Component Adsorption Results

Component	**N_{exp}**	**Experimental T (K)**	**Experimental P range (MPa)**	**δ_p/σ**	**ε_p (K)**	**Reference**	**ARD (%)**
Methane	7	303.15	1×10^{-2} - 5	0.2426	947.28	Nieto-Draghi *et al.*[26]	8.56
Carbon dioxide	7	303.15	1×10^{-2} - 5	0.2931	1089.18	Nieto-Draghi *et al.*[26]	9.03

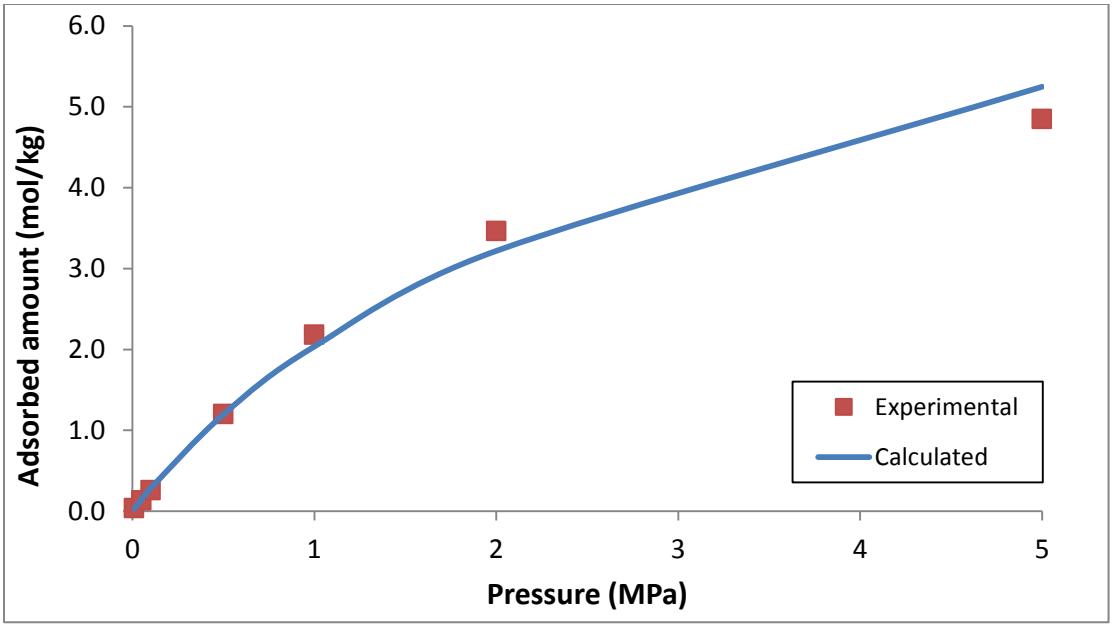

Figure 19: Calculated versus experimental results for methane adsorbed in ZIF-8 (SOD) at 303.15 K (Nieto-Draghi *et al.*)[26]

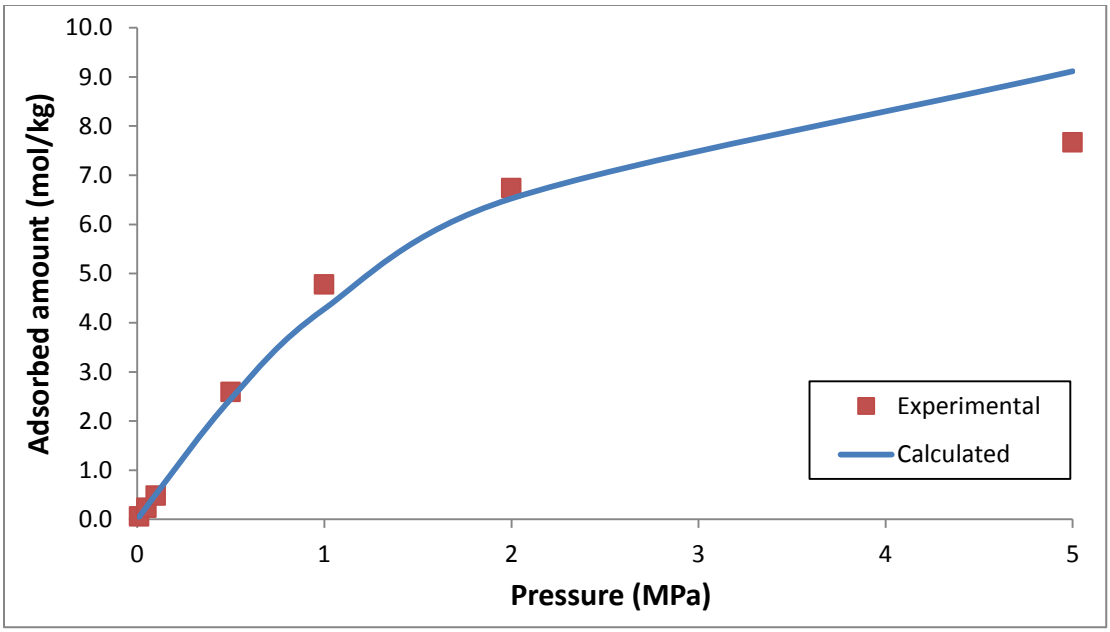

Figure 20: Calculated versus experimental results for carbon dioxide adsorbed in ZIF-8 (SOD) at 303.15 K (Nieto-Draghi *et al.*)[26]

Mixtures

Figure 21 shows the results of the adsorption of the methane and carbon dioxide mixture in ZIF-8 at 303.15 K. The mole fractions of methane and carbon dioxide in the bulk phase are equal to 0.75 and 0.25, respectively, in all experimental data points. The fitted k_{12} (=k_{21}) value is 0.383. The model captures the general trend of the experimental data except for the apparent change in selectivity at the highest experimental pressure of 5 MPa.

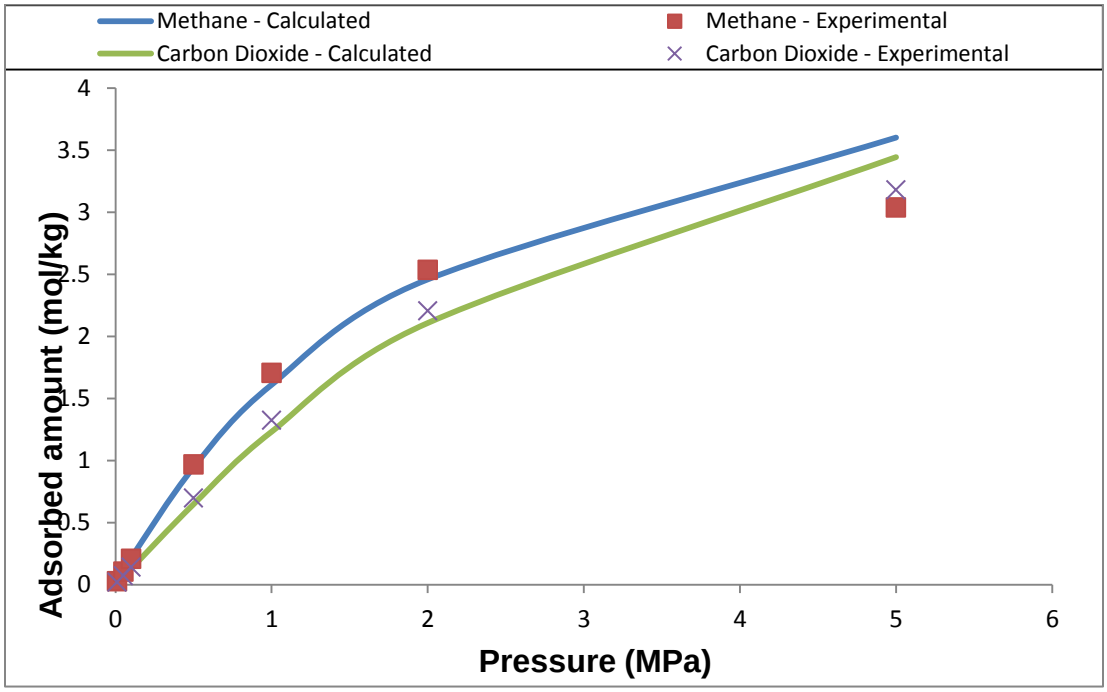

Figure 21: Calculated versus **e**xperimental results for a mixture of methane and carbon dioxide adsorbed in ZIF-8 (SOD) at 303.15 K, fitted k_{12} value of 0.383 (Nieto-Draghi *et al.*)[26]

Chabazite Results

Pure Components

The adsorption of methane and carbon dioxide in chabazite was also studied. The diameter of the chabazite adsorbent pores is 3.8 Å according to Li *et al.*[27], which is much smaller in comparison to both zeolite A and sodalite. However, there are several reported values for the diameter of this adsorbent and a diameter of 8 Å, from ZEOMICS[17] was adopted. It was presumed that due to less space available within the pore, the effects of confinement would be more pronounced, thus it could possibly affect the outcome. The results for chabazite are summarized in Table 8.

Table 8: Chabazite Pure Component Data

Component	**N_{exp}**	**Experimental T (K)**	**Experimental P range (MPa)**	**δ_p/σ**	**ε_p (K)**	**Reference**	**ARD (%)**
Methane	9	297.15	1.2×10^{-2} – 1.1×10^{-1}	0.21063	1293.934	Li *et al.*[27]	16.96
Carbon dioxide	10	297.15	1.2×10^{-2} – 1.1×10^{-1}	0.44662	1769.982	Li *et al.*[27]	2.98

Figure 22 shows the results for methane, for which the ARD is 16.96%. Despite this apparently high ARD value, the calculated results show very acceptable behavior, taking into account the scattering of the experimental information. The experimental data of carbon dioxide exhibit much less scattering. The calculated values agree well with the experimental information, and the ARD value is 2.98%.

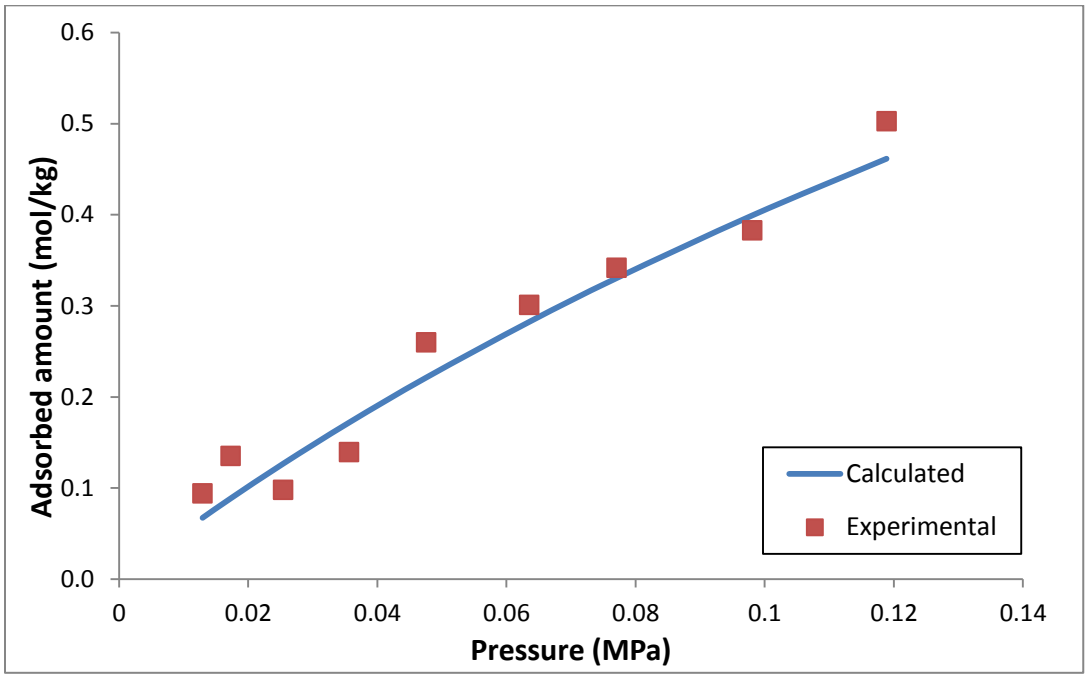

Figure 22: Calculated versus experimental results for methane adsorbed in chabazite (SSZ-13) at 297.15 K (Li *et al.*)[27]

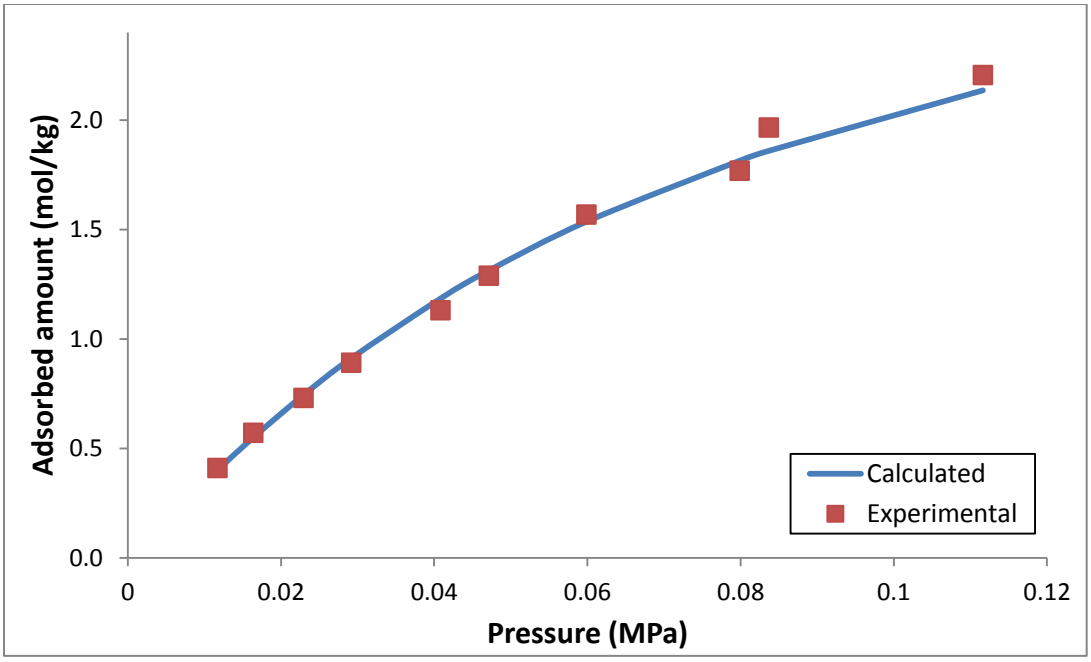

Figure 23: Calculated versus experimental results for carbon dioxide adsorbed in chabazite (SSZ-13) at 297.15 K (Li *et al.*)[27]

The average occupancy number for the pure components at the highest experimental bulk phase pressure are predict to be only 0.32 molecules for methane and 1.5 molecules for carbon dioxide are adsorbed. However, the molecular diameter of carbon dioxide is bigger than that of methane. Hence, there is a possibility of a higher preference for the adsorption of carbon dioxide molecules as opposed to methane.

Mixtures

In the case of the methane and carbon dioxide mixture in chabazite depicted in Figure 24, the calculated results for methane predict the experimental trend very well, whereas the carbon dioxide trend is not as good qualitatively.

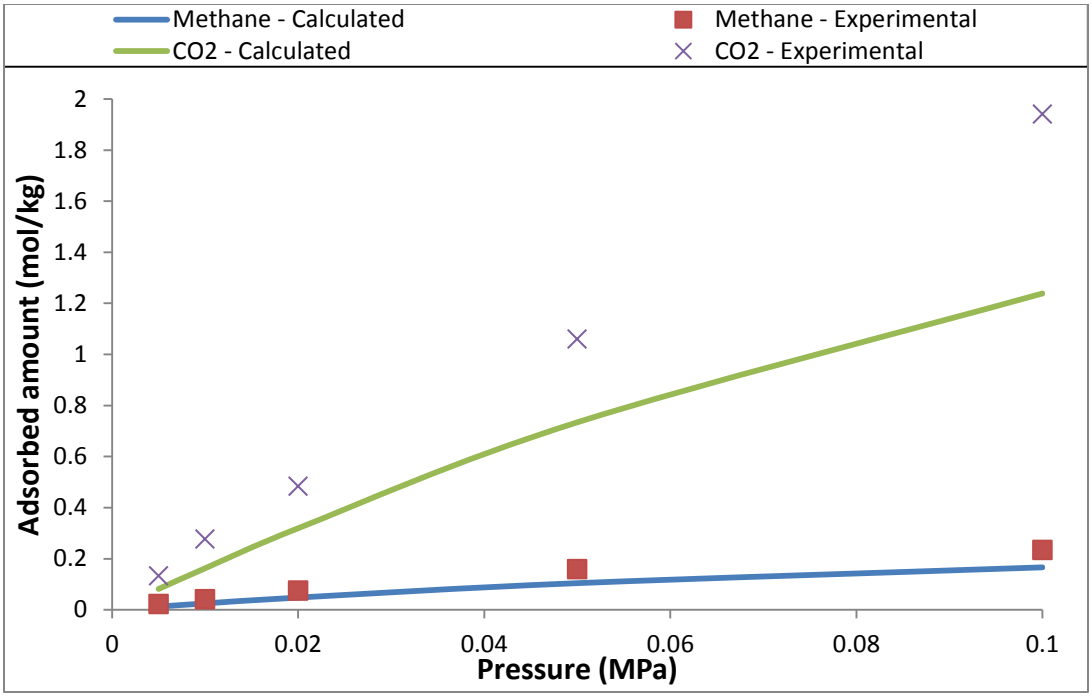

Figure 24: Calculated versus experimental results for a mixture of methane and carbon dioxide adsorbed in chabazite (SSZ-13) at 297K, fitted k_{ij} value of 0 (Li *et al.*)[27]

The fitted k_{12} value is found to be approximately zero, but this is due to the fact that its value was constrained to be non-negative. Without the use of a constraint, the k_{12} value is found to be -2.4, but this does not bring substantial improvement to the model's representation of carbon dioxide behavior.

CHAPTER VII

CONCLUSIONS

In order to model fluids confined in porous media with spherical pores, the generalized van der Waals theory was applied to modify the Peng-Robinson equation of state. The developed model contains two adjustable parameters for each component of fluid. These parameters are related to the interactions between the fluid molecules and the pore walls. The effect of pore size on the properties of the fluid was explicitly represented in the model. This enables it to describe the behavior of fluids in pores of different sizes, in both the bulk and confined state, and with the same values of its parameters. Thus, the same model can be applied to all the phases of adsorption systems. Although not studied in this thesis, the model can also be used to derive expressions for calorimetric properties such as residual enthalpy, which is convenient for energy balances in adsorption systems.

The model is intended to describe the average behavior of many molecules distributed inside many pores. It is not meant for and is not capable of predicting the spatial distribution of the molecules inside a pore, in the same way that a conventional equation of state for bulk fluids is not intended to predict the spatial distribution of molecules in a bulk phase.

One aspect that must be taken into careful consideration is the source of the experimental data. Adsorption isotherm experiments are complex and have a large room for uncertainty, as the data used in some of the applications illustrated. Since the

modeling is dependent on parameter fitting from experimental data, unreliable data is likely to yield poor results. In addition, in the adsorption literature, it is common to find articles that only present the experimental data in plots. Extracting numerical values from them adds to the uncertainty. Therefore, the data should preferably come from reliable sources where they appear in tabular form. On a similar note, it is also important to source pure component data and mixture data from the same experimental set-up, as different experimental set-ups can give origin to data discrepancies between seemingly similar systems.

Average relative deviations (ARDs) between the experimental and calculated results, as well as the average occupancies, were used to assess the model's performance. For the pure component adsorption cases studied in this work, the ARD was slightly larger than 20% in two cases, between 10% and 20% in three cases, between 5% and 10% in four cases, and below 5% in three cases. However, these numbers should be used with care. In some of the cases, there is clear systematic deviation between experimental and calculated results. In at least one case, such as methane adsorption in chabazite, the ARD value seems to be related to the scattering of the experimental data rather than the model's inability to represent the system. The average occupancy numbers predicted by the model are lower than the maximum theoretical occupancy. Hence, with respect to the examples provided in this thesis, there is no violation of the theoretical limit of molecules that can be adsorbed. For mixtures, the generally accepted values for the binary interaction parameter (k_{ij}) of cubic equations of state for bulk fluids lie within the range of 0 to 1, but that is not the case for this

model. The fitted k_{ij} parameters exceed this limit considerably, but have proven to be necessary to provide better fits for the calculated data.

The model showed a tendency to overestimate adsorbed amounts of pure components at high values of the bulk phase pressure. The corresponding pressure values inside the pores are even higher. This poor prediction at high pressures suggests that there may be a flaw with the expression developed for free volumes. At such conditions, it is possible that the repulsive term of the model, based on van der Waals free volume expression, could be a contributing factor towards why the model cannot predict saturation at higher pressures. The high pressures experienced in the confined phase may push the free volume expression well past its limiting application condition. Future refinements could result from using a modified version of the Carnahan-Starling expression for the repulsive part, to account for the effect of confinement.

Future work will have to expand this performance analysis by including other adsorption models. In addition, there are several possible modifications and extensions, which are discussed in the next chapter.

CHAPTER VIII

FUTURE WORK

This work can be extended in a number of directions, which are outlined in this chapter.

Additional comparisons are necessary for a complete assessment of the model's potentials and limitations. The experimental data need to be selected very carefully, and especially when dealing with mixtures. Both the pure component and mixture data should preferably come from the same source. The current results suggest that the model overestimates the adsorbed amounts of pure components at high pressures, but more evidence is needed to reach a conclusion.

There are several advantages associated with using a single model which is applicable to both confined and unconfined fluids, and is derived from the canonical partition function, as it can be the single source for the expressions of all thermodynamic properties. This is theoretically convenient, but the ultimate test for models is their comparison to experiments. Future work should focus on testing the model with more substances, mixtures, and different adsorbents, and comparison of its performance to that of other adsorption models. Future work would also entail the calculation of heats of adsorption, based on the equations developed in this thesis.

It would be interesting to combine the models for confinement in cylindrical and spherical pores to predict adsorption behavior in zeolites that have both kinds of pores present. The results could then be compared to the separate spherical and cylindrical

results, to determine which representation is more accurate. This research could extend to the simulation of adsorption equilibrium in heterogeneous porous adsorbents, in which the presence of both cylindrical and spherical pores is prominent. Furthermore, the developed model can be inserted into a general flash program, which has the capability of automatically determining the number of bulk and confined phases in equilibrium. This type of calculation has already been implemented for adsorbents with cylindrical pores, with meaningful results.

In this thesis, all the calculations involved systems with small pores, with diameters of about 10 Å. As the results for average occupancy showed, few molecules are predicted to be inside such pores. This is possibly the most stringent test for the developed model. It will be interesting to test how it performs for mesoporous systems (typical pore diameters from 2 to 50 nm), which could have better functionality.

With respect to industrial applications, a field of further interest is that of shale oil, where kerogen is trapped in tight rock formations. Shale oil is poised to become North America's largest source of energy, due to large deposits that have been located in the Green River formation situated in Colorado, Utah and Wyoming, as well as in the Barnett Shale and Eagle Ford Shale formations in Texas. It is estimated that the recoverable amount of shale oil in the Green River formation exceeds 800 billion barrels[28], while the maximum production of the Eagle Ford formation could reach 800,000 barrels a day[29].

While there is future potential for mass production of shale oil, it is still an area that remains to be explored. Extraction of shale oil is extremely complex, and requires

expensive heating and refining processes. Further applications of the equation for confinement could extend to shale oil, possibly extended to confinement in pores of different shapes, in order to describe the behavior of the confined deposits by providing necessary information such as the confined pressures. For example, Marcellus shale[30] found in the Appalachian basin is comprised of several flat plates, which could be a possible structure to explore in the future. Several properties such as pressure, density and compositional grading due to gravitational effects could be determined through use of a similar thermodynamic model. Such studies can help in the facilitation of better suited shale oil extraction techniques.

REFERENCES

1. Warrag, S., *A Thesis on Multiphase Equilibrium of Fluids Confined in Fischer-Tropsch Catalytic Systems,* Texas A&M University at Qatar; 2014.
2. Travalloni, L., Castier, M., Tavares, F. W., Sandler, S. I., Thermodynamic Modeling of Confined Fluids Using an Extension of the Generalized van der Waals Theory. *Chem. Eng. Sci.* 2010;65(10):pp. 3088-3099.
3. Zhu, H. Y., Ni, L. A., Lu, G. Q., A Pore-size-dependent Equation of State for Multilayer Adsorption in Cylindrical Mesopores. *Langmuir.* 1999;15(10):pp. 3632-3641.
4. Schoen, M., and Diestler, D. J., Analytical Treatment of a Simple Fluid Adsorbed in a Slit-Pore. *J. Chem. Phys.* 1998;109(13):pp. 5596-5606.
5. Truskett, T. M., Debenedetti, P. G., Torquato, S., Thermodynamic Implications of Confinement for a Waterlike Fluid. *J. Chem. Phys.* 2000;114(5):pp. 2401-2418.
6. Giaya, A., and Thompson, R., Water Confined in Cylindrical Micropores. *J. Chem. Phys.* 2002;117(7):pp. 3464-3475.
7. Zarragoicoechea, G. J., and Kuz, V. A., Critical Shift of a Confined Fluid in a Nanopore. *Fluid Phase Equilib.* 2004;220(1):pp. 7-9.
8. Derouane, E. G., On the Physical State of Molecules in Microporous Solids. *Microporous Mesoporous Mater.* 2007;104(1-3):pp. 46-51.

9. Sandler, S. I., The Generalized van der Waals Partition Function. I. Basic Theory. *Fluid Phase Equilib.* 1985;19(3):pp. 238-257.

10. Woods, G. B., Panagiotopoulos, A. Z., Rowlinson, J. S., Adsorption of Fluids in Model Zeolite Cavities. *Mol. Phys.* 2000;63(1):pp. 49-63.

11. Hill, T. L., *An Introduction to Statistical Thermodynamics.* New York: Dover Publications; 1960.

12. Pfoertner, H., Densest Packing of Spheres in a Sphere. 2011; http://www.randomwalk.de/sphere/insphr/spheresinsphr.html.

13. Richards, F. J., A Flexible Growth Function for Empirical Use. *J. Exp. Bot.* 1959;10(2):pp. 290 - 301.

14. Casella, G., and Berger, R. L., *Statistical Inference.* 2 ed. Belmont, CA: Duxbury Press; 1990.

15. Travalloni, L., Castier, M., Tavares, F. W., Phase Equilibrium of Fluids Confined in Porous Media from an Extended Peng-Robinson Equation of State. *Fluid Phase Equilib.* 2014;362:pp. 335-341.

16. Onken, U., Rareynies, J., Gmehling, J., The Dortmund Data Bank - A Computerized System for Retrieval, Correlation, and Prediction of Thermodynamic Properties of Mixtures. *Int. J. Thermophys.* 1989;10(3):pp. 739-747

17. First, E. L., and Floudas, C. A., ZEOMICS - Zeolites and Microporous Structures Characterization. 2011; http://helios.princeton.edu/zeomics/.

18. Macedo, R. S., Alfredique, M. F., Castier, M., Automatic Generation of Matlab Functions using Mathematica and Thermath. *Comput. Sci. Eng.* 2008;10(4):pp. 41-49.

19. Castier, M., XSEOS - An Open Software for Chemical Engineering Thermodynamics. 2011.

20. Topliss, R. J., Dimitrelis, D., Prausnitz, J. M., Computational Aspects of a Non-cubic Equation of State for Phase-Equilibrium Calculations: Effect of Density-Dependent Mixing Rules. *Comput. Chem. Eng.* 1988;12(5):pp. 483-489.

21. Sievers, W., *Uber das Gleichgewicht der Adsorption in Anlagen zur Wasserstoff gewinnung [A Thesis about the Equilibrium of Adsorption in Systems for Hydrogen Recovery]*, Technische Universitat München; 1994.

22. Loughlin, K. F., Hasanain, M. A., Abdul-Rehman, H. B., Quaternary, Ternary, Binary, and Pure Component Sorption on Zeolites. 2. Light Alkanes on Linde 5A and 13X Zeolites at Moderate to High Pressures. *Ind. Eng. Chem. Res.* 1990;29(7):pp. 1535-1546.

23. Glessner, A. J., and Myers, A. L., Sorption of Gas Mixtures in Molecular Sieves. *Elsevier.* 1969;65 (96):pp. 73-79.

24. Grande, C., and Gigola, A., Adsorption of Propane and Propylene in Pellets and Crystals of 5A Zeolite. *Ind. Eng. Chem. Res.* 2002;41(1):pp. 85-92.

25. Hirschfelder, J. O., Curtiss, C. F., Bird, R. B., *Molecular Theory of Gases and Liquids.* Vol 120. New York: Wiley; 1954.

26. Nieto-Draghi, C., Amrouche, H., Aguado, S., Perez-Pellitero, J., Chizallet, C., Siperstein, F., Farrusseng, D., Bats, N., Experimental and Computational Study of Functionality Impact on Sodalite-Zeolitic Imidazolate Frameworks for CO_2 Separation. *J. Phys. Chem.* 2011;115(33):pp. 16425-16432.

27. Li, S., Noble, R., Falconer, R. D., Improved SAPO-34 Membranes for CO2/CH4 Separations. *Adv. Mater.* 2006;18(19):pp. 2601-2603.

28. Environmentally Conscious Consumers for Oil Shale, Oil Shale in Colorado, Utah and Wyoming. 2011; http://www.eccos.us/oil-shale-in-co-ut-wy.

29. Blackmon, D., Texas's Amazing Shale Oil And Gas Abundance. 2013; http://www.forbes.com/sites/davidblackmon/2013/07/05/texass-amazing-shale-oil-and-gas-abundance/.

30. Curtis, R., What is Marcellus Shale? 2011; http://energy.wilkes.edu/pages/152.asp.

APPENDIX

Explanation of Functions used in the Code

The Thermath[18], Matlab and Visual Basic developed code is used to calculated pressure and its first two derivatives with respect to molar volume at constant temperature for pure components, i.e.

$$\left(\frac{dP}{dV}\right)_T \; and \; \left(\frac{d^2P}{dV^2}\right)_T = 0, \text{ at the critical point}$$

The main functions concerned are *prslnphiv*, which is the fugacity coefficient for vapor, *prslnphil*, the fugacity coefficient for liquid and *prsvv*, the molar volume. All three functions rely on the *eospropspspec* function which is defined as,

$$eospropspspec(kual\_eos, propset, ifase, rcell, Tcell, Pcell, xcells,$$

$$parametercells, extracells)$$

It takes the program-defined parameters *kual_eos*, which refers to the equation of state under consideration, *propset*, which distinguishes between fugacity coefficients and molar volume, and *ifase*, which is a part of a procedure created by Topliss *et al*.[20] For the modified Peng-Robinson equation of state, *kual_eos* is assigned a value of 13. For liquids, the *ifase* value is 1, and for vapor, the *ifase* value is -1. *Propset* is assigned a value of 1 for fugacity coefficients and 4 for molar volume. The *eospropspspec* function also takes values inputted by the user, such as the gas constant *rcell*, temperature *Tcell*, pressure *Pcell*, mole fraction *xcells*, the critical properties of the substance *parametercells*, and any additional values go into *extracells*. In addition to these parameters, there also exists the *eosget* variable which calls the equation of state routine,

and the *preos* variable which calls various routines needed to calculate properties for the Peng-Robinson equation of state for adsorption in spherical pores. Molar density is calculated on the basis of either the *brootforce* or the Topliss *et al.*[20] technique. *Brootforce* is essentially a method by which brute force is applied to make the routine work.